NASA Technical Memorandum 86373

NASA-TM-86373 19850010912

Broad-Band UHF Dipole Array

M. C. Bailey

February 1985

National Aeronautics and
Space Administration

Langley Research Center
Hampton, Virginia 23665

BROAD-BAND UHF DIPOLE ARRAY

by
M. C. Bailey

Summary

A 6X6 array of fan-dipoles has been designed to operate in the 510 to 660 MHz frequency range for aircraft flight test and evaluation of a UHF radiometer system. Details of a broad-band dipole design operating near the first resonance is described. Measured VSWR and radiation patterns for the dipole array demonstrate achievable bandwidths in the 35 to 40 percent range.

Introduction

The antenna described in this paper was developed for the aircraft flight test and evaluation of an ultrahigh frequency (UHF) radiometer system. The radiometer was designed with the capability of selecting one of several frequency bands within the 510 to 660 MHz range, thus the antenna was required to present a good impedance match and low-sidelobe radiation patterns over a wide frequency band. The purpose of the present paper is to provide details of the broadband antenna array design.

Antenna Description

During flight testing of the radiometer, the antenna was to be installed in the forward bomb-bay of a P-3 Orian aircraft. Due to restrictions on the height of the antenna and the radiometer requirements for low sidelobes (high beam-efficiency), an array antenna appeared to be a logical approach for this application. Since the bomb-bay opening could accommodate only about a 3.0λ to 3.5λ wide antenna at UHF, a 6X6 array of 0.5λ spaced elements was selected as the basic antenna. This would allow some flexibility for tapering the amplitude excitation for low sidelobes while maintaining an even number of elements for ease of feed network distribution design. The most challenging aspect of the design was to develop an element whose maximum dimension is less than 0.5λ and whose bandwidth is greater than 25 percent.

A sketch of the antenna concept is illustrated in figure 1. The antenna is a 6X6 array of fan-dipoles with a stripline corporate feed network designed so as to approximate a cosine excitation distribution in orthogonal directions.

The fan-dipole is illustrated in figure 2 and photographs of one element are presented in figures 3 and 4. The fan-dipole consists of two equilateral triangular sheets of copper etched on one side of a teflon-fiberglass printed-circuit board and excited by a 50Ω semi-rigid coax cable. The outer conductor of the coax and an adjacent coax serve as a balanced-to-unbalanced impedance matching transformer. The printed-circuit board provides mechanical support for the triangular arms of the dipole. The loading effect of the printed-circuit board was determined to be insignificant at UHF. A fiberglass enclosure (with access openings) provides mechanical support for the

printed-circuit board. The effect upon the impedance and radiation properties of the fiberglass enclosure was also determined to be insignificant. Details of the dipole design will be given in a later section.

The feed network is an assemblage of several stripline panels with coax cable interconnections between the three layers of printed-circuit boards. The feed network (illustrated in figure 5) is a combination of 3-way unequal power-dividers and a 4-way equal power-divider. The implementation of the circuit in stripline was accomplished in three layers of printed-circuit boards. The first layer stripline circuit is illustrated in figure 6 as twelve 3-way power-dividers, the second layer is illustrated in figure 7 as four 3-way power-dividers, and the third layer is illustrated in figure 8 as a 4-way divider. The stripline circuits for each layer are configured such that the points of interconnection between layers occur immediately over the corresponding points for each layer. These interconnections were implemented with short straight sections of semi-rigid coax cable.

A photograph of the back side of the array is shown in figure 9 with half of the first layer printed-circuit boards installed. The front side of the array is shown in figure 10 with the 36 fan-dipole elements installed. A front view of the final array is shown in figure 11. The foam inserts (located between the dipoles) support thin sheets of conductive foil which serve as isolation baffles to reduce the mutual coupling between array elements. It was found during the development stage that these baffles improved the impedance match across the design bandwidth at the input to the complete antenna assembly.

Dipole Element

The broad-band dipole element was designed by an experimental parametric study of the impedance characteristics versus the element length and height. The parameters of interest are illustrated in figure 12. Starting with an initial design (L=14.526cm, H=12.7cm) which was tuned to mid-band, the length and height were adjusted to maximize the bandwidth of the element. An increase in the height of the dipole above the ground plane (with a corresponding increase in the length of the balun) tends to increase the bandwidth, as indicated in figure 13. This increase in bandwidth is also accompanied by a

shift of the center frequency to a higher value, thus requiring an increase in element length in order to lower the center frequency back to the desired range. Since increasing the element length also reduces the bandwidth, as shown in figure 14, additional dipole height is necessary in order to match the antenna impedance to 50Ω over a wide frequency band while keeping the center frequency within the desired range, as shown by the data in figure 15. Further iterations of length and height should result in an optimized design.

The measured input voltage standing-wave ratio (VSWR) for the final dipole design is shown in figure 17. The final results were improved slightly by making one arm of the dipole slightly shorter than the other. Apparently the strip connecting the arm to the coax center conductor effectively increases the length of this arm and should be taken into consideration if one should desire to scale the present design to another frequency band. The final dipole design achieved a VSWR less than 1.5:1 over a 25 percent bandwidth and a VSWR less than 2:1 over a 37 percent bandwidth.

The repeatability of the design is demonstrated in figure 17 where the reflection coefficient versus frequency of all 36 dipole elements is plotted. The shaded area in figure 17 indicates the maximum variation between the 36 plots.

It is anticipated that the radiation pattern of a fan-dipole can be adequately modeled for design purposes by a linear dipole with a cosine current distribution. The principal plane patterns for a horizontal linear dipole over an infinite conducting ground plane can be calculated from

E-plane:

$$E_\theta = \frac{\sin(2\pi H/\lambda \cos\theta)\,[\cos(\pi L/\lambda \sin\theta) - \cos(\pi L/\lambda)]}{[1 - \cos(\pi L/\lambda)]\cos\theta} \qquad (1)$$

H-plane:

$$E_\phi = \sin(2\pi H/\lambda \cos\theta) \qquad (2)$$

where L is the length of the dipole, H is the height above the ground plane, and λ is the wavelength at the operating

frequency. Equations 1 and 2 are plotted in figure 18 for L=16.2cm and H=19.4cm at the center frequency of the design band and at the band edges. A depression in the pattern occurs as the frequency increases due to the increase in height (in wavelengths). This depression should become a null for higher frequencies because of phase cancellation from the dipole image as the height approaches $\lambda/2$. The allowable depth of the depression will limit the usable upper frequency of the dipole.

The measured radiation patterns (figures 19-25) demonstrate the pattern bandwidth characteristics of the dipole located in the center of a 122cm by 122cm ground plane. There are some effects observed in the measured patterns due to the finite size of the ground plane. If desired, these effects can be modeled analytically by including the electromagnetic scattering from the ground plane edges in the calculations. In symbolic notation, the finite ground plane effects upon the radiation patterns can be accounted for by

E-plane:

$$E_\theta = E_\theta^o + E_\theta^r + E_h^d + E_h^{sd} + E_\theta^c \qquad (3)$$

H-plane:

$$E_\phi = E_\phi^o + E_\phi^r + E_s^d + E_s^{sd} + E_\phi^c \qquad (4)$$

where E_θ^o and E_ϕ^o represent the radiation pattern of a dipole in free space, E_θ^r and E_ϕ^r represent the reflected field or radiation pattern of the dipole image, E_h^d and E_s^d represent the edge diffracted fields, E_h^{sd} and E_s^{sd} represent a correction to the edge diffracted fields due to the slope of the field illuminating the edges, and E_θ^c and E_ϕ^c represent the field scattered from the corners of the ground plane. The reader is referred to the literature [1,2,3] for more detailed explanation of edge scattering and the mathematical expressions for the terms in equations 3 and 4.

Calculations of the E-plane and H-plane patterns for a dipole over a finite ground plane are compared in figure 26

with measured patterns of the fan-dipole. The comparison in figure 26 demonstrates that the fan-dipole can be adequately modeled as a linear dipole. The edge effects of the finite ground plane should be less important for the array design since the feed network is designed so as to produce a null in the array factor along the ground plane (90° from broadside); therefore, the ground plane diffraction effects will be neglected. This assumption will be verified later by comparison between the measured radiation patterns of the fan-dipole array and calculations for an array of linear dipoles on an infinite ground plane.

Power Dividers

The excitation distribution feed networks are implemented in stripline using two teflon-fiberglass printed circuit boards of 0.159cm thickness. As an intermediate step in the design, stripline power dividers utilizing 1.5λ hybrids were designed, fabricated, and tested. The stripline circuit for one of the 3-way unequal power dividers is illustrated in figure 27. The 3-way divider was designed so as to approximate one side of a cosine distribution at the 3 output ports. Measured transmission and reflection properties of the 3-way divider are presented in figure 28 over the frequency band of the radiometer. The stripline circuit for the 4-way equal power divider is illustrated in figure 29 and the measured transmission and reflection properties are presented in figure 30. The measurements in figures 28 and 30 indicate that the feed network design concept with good wideband characteristics may be feasible.

Results

After assembly of the antenna and feed network, the input impedance match was not as good as anticipated. The measured reflection coefficient at the input to the assembly is shown by the dashed curve in figure 31. An attempt was made to improve the input impedance match by reducing the H-plane interelement coupling of the dipoles through use of conducting fences of 20.32cm height between rows of dipoles. The resultant improvement is illustrated by the solid curve in figure 31.

The measured input VSWR for the final antenna (with baffles installed) is presented in figure 32. The antenna array exhibits an impedance bandwidth (VSWR<2:1) of better than 40 percent.

The measured radiation patterns for the final antenna (at the center frequency of the radiometer band) are compared with calculated patterns for an array of linear dipoles (with a cosine excitation distribution) located over an infinite ground plane. The radiation patterns agree quite well except for the H-plane wide-angle sidelobe levels and this difference is probably due to neglecting the ground plane edge scatter in the element pattern calculations.

The pattern bandwidth characteristics for the final antenna assembly are illustrated by the measured principal plane patterns in figures 34-37. These results demonstrate the wideband low-sidelobe properties of the antenna design. Measured radiation patterns outside the 500-710 MHz band are not available; therefore, the full pattern bandwidth is undetermined.

Conclusions

A UHF dipole array with wideband impedance and low-sidelobe properties has been designed, fabricated and tested. Measured bandwidths in the 35 to 40 percent range have been demonstrated.

References

1. R. G. Kouyoumjian and P. H. Pathak, "A Uniform Geometrical Theory of Diffraction for an Edge in a Perfectly-Conducting Surface," Proc. IEEE, Vol. 62, November 1974, pp. 1448-1461.

2. R. G. Kouyoumjian, "The Geometrical Theory of Diffraction and Its Applications," Numerical and Asymptotic Techniques in Electromagnetics, edited by R. Mittra, Spring-Verlag, New York, 1975.

3. W. D. Burnside, N. Wang and E. L. Pelton, "Near Field Pattern Computations for Airborne Antennas," OSU Report 4685-4, The Ohio State University ElectroScience Laboratory, June 1978.

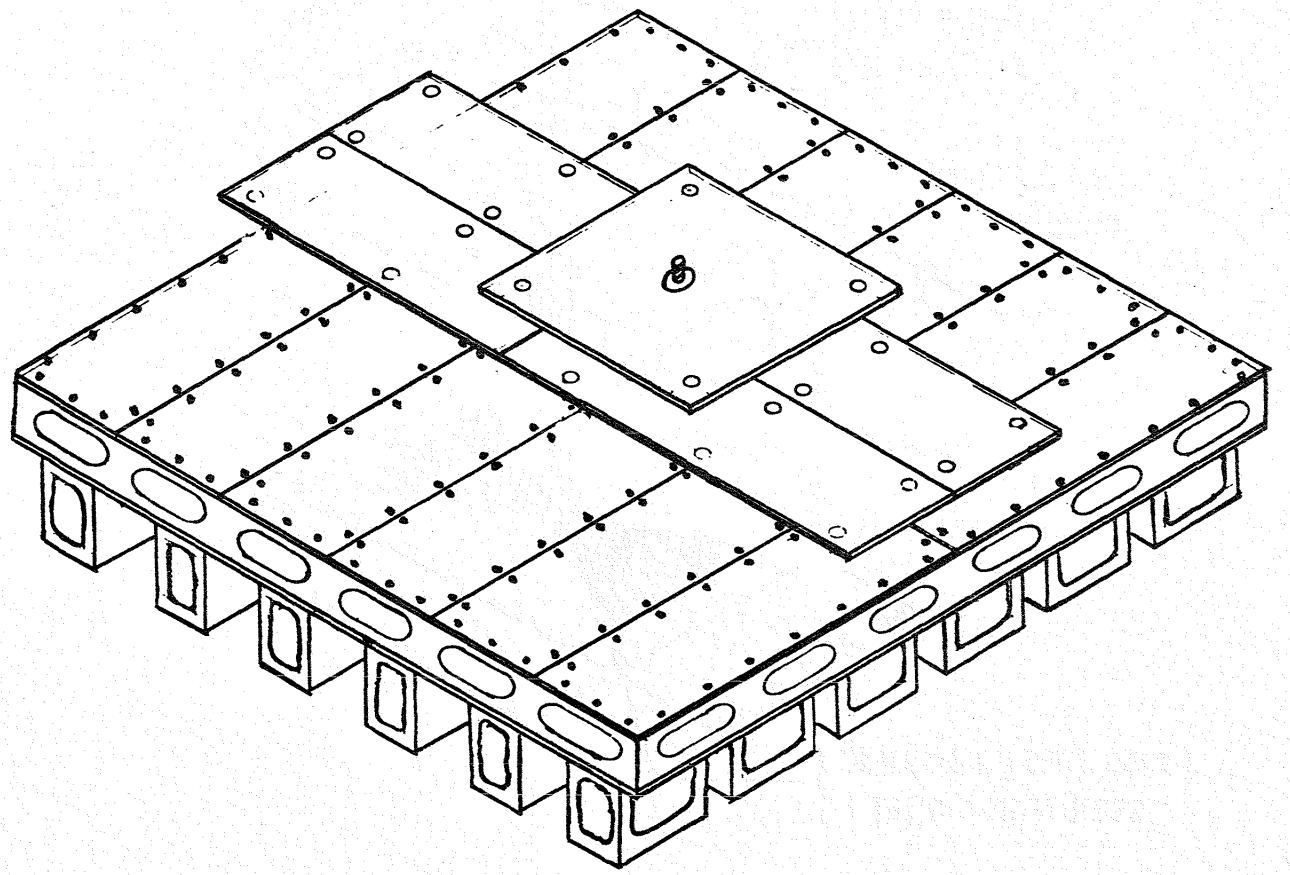

Figure 1. Sketch of broad-band low-sidelobe UHF array.

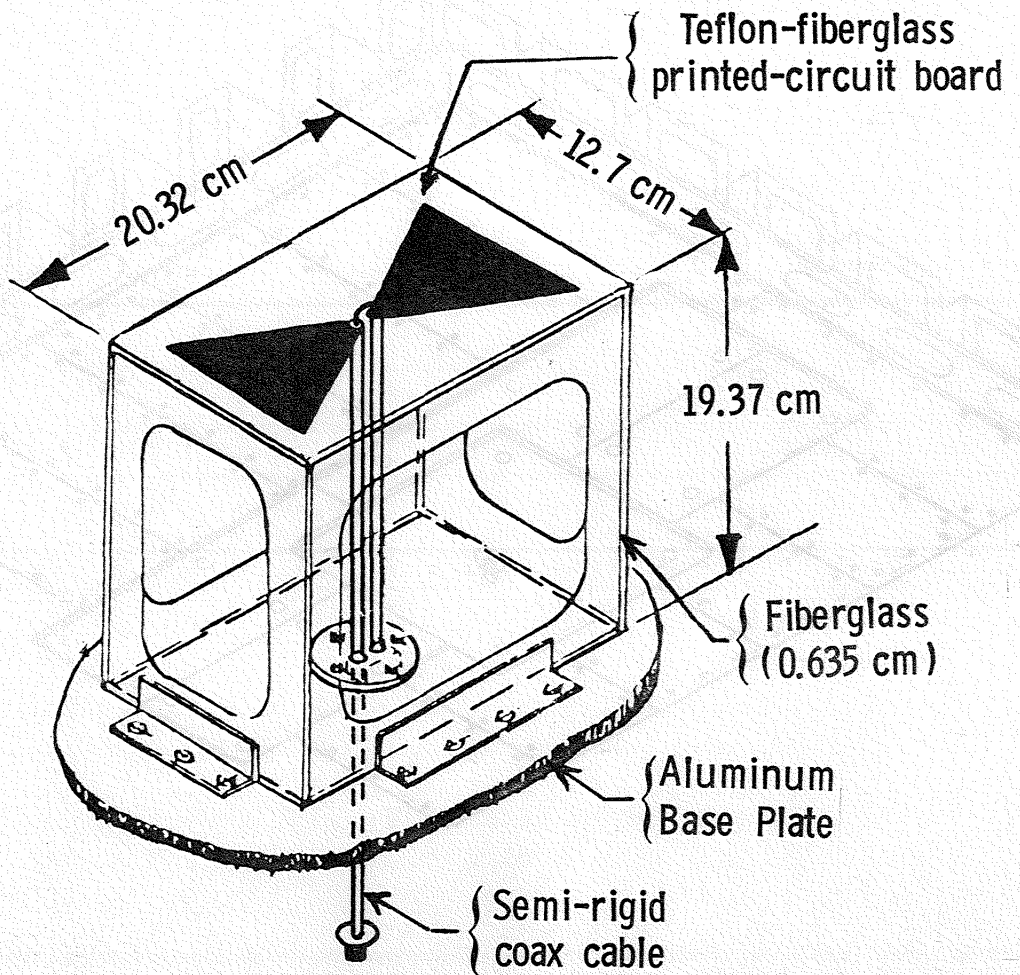

Figure 2. Sketch of broad-band UHF dipole.

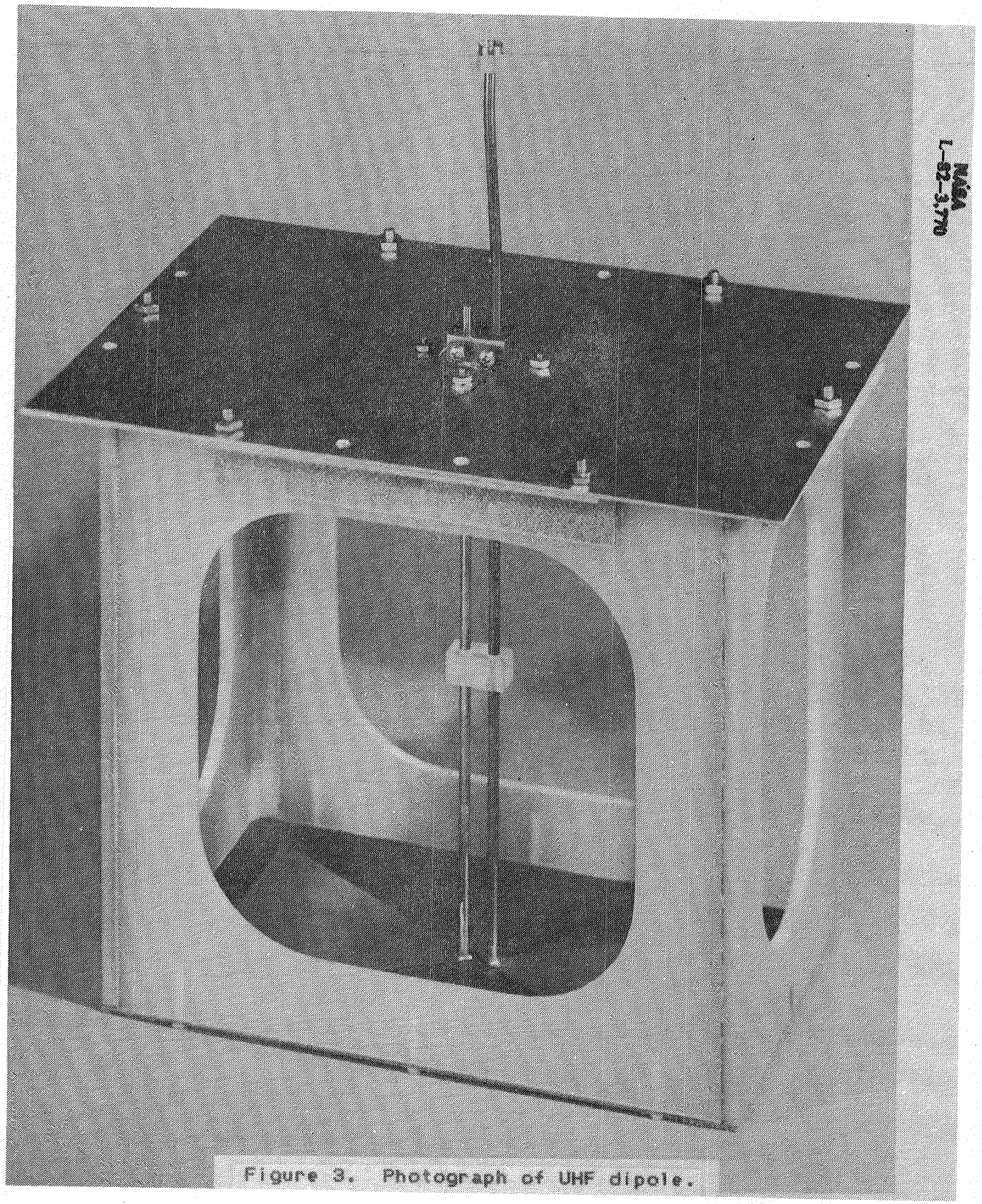

Figure 3. Photograph of UHF dipole.

NASA
L-82-3,769

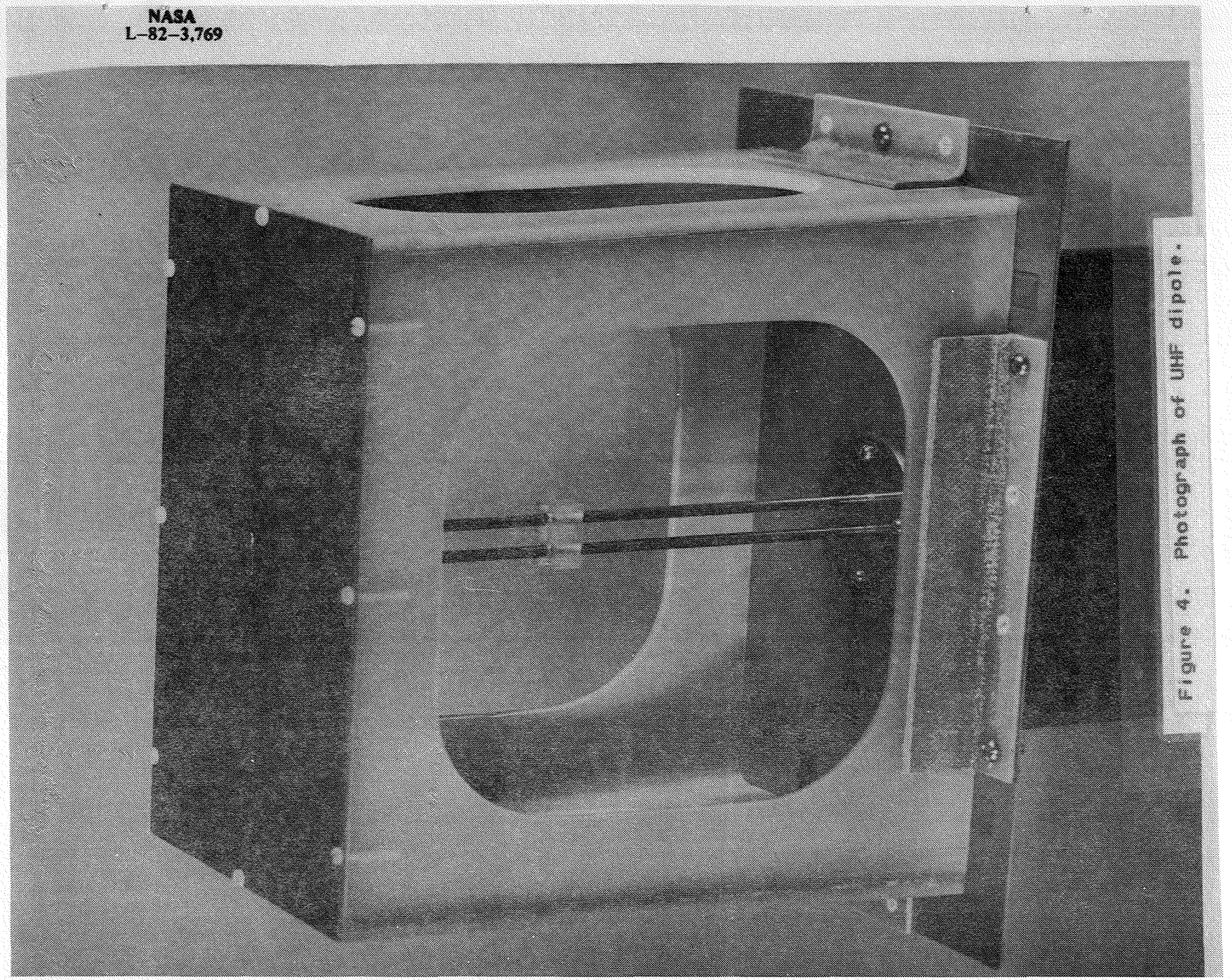

Figure 4. Photograph of UHF dipole.

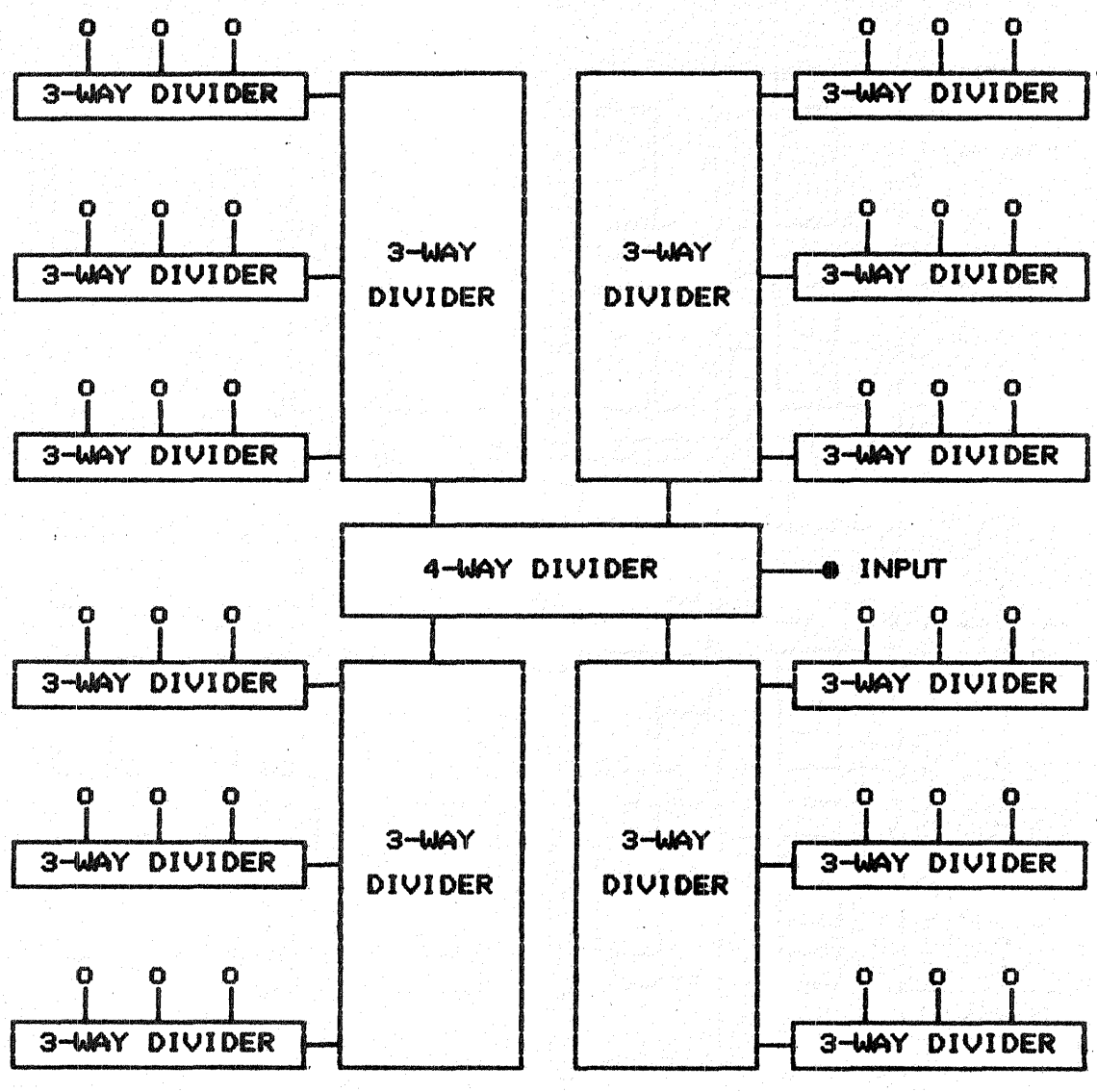

Figure 5. Block diagram of feed network for 6X6 array.

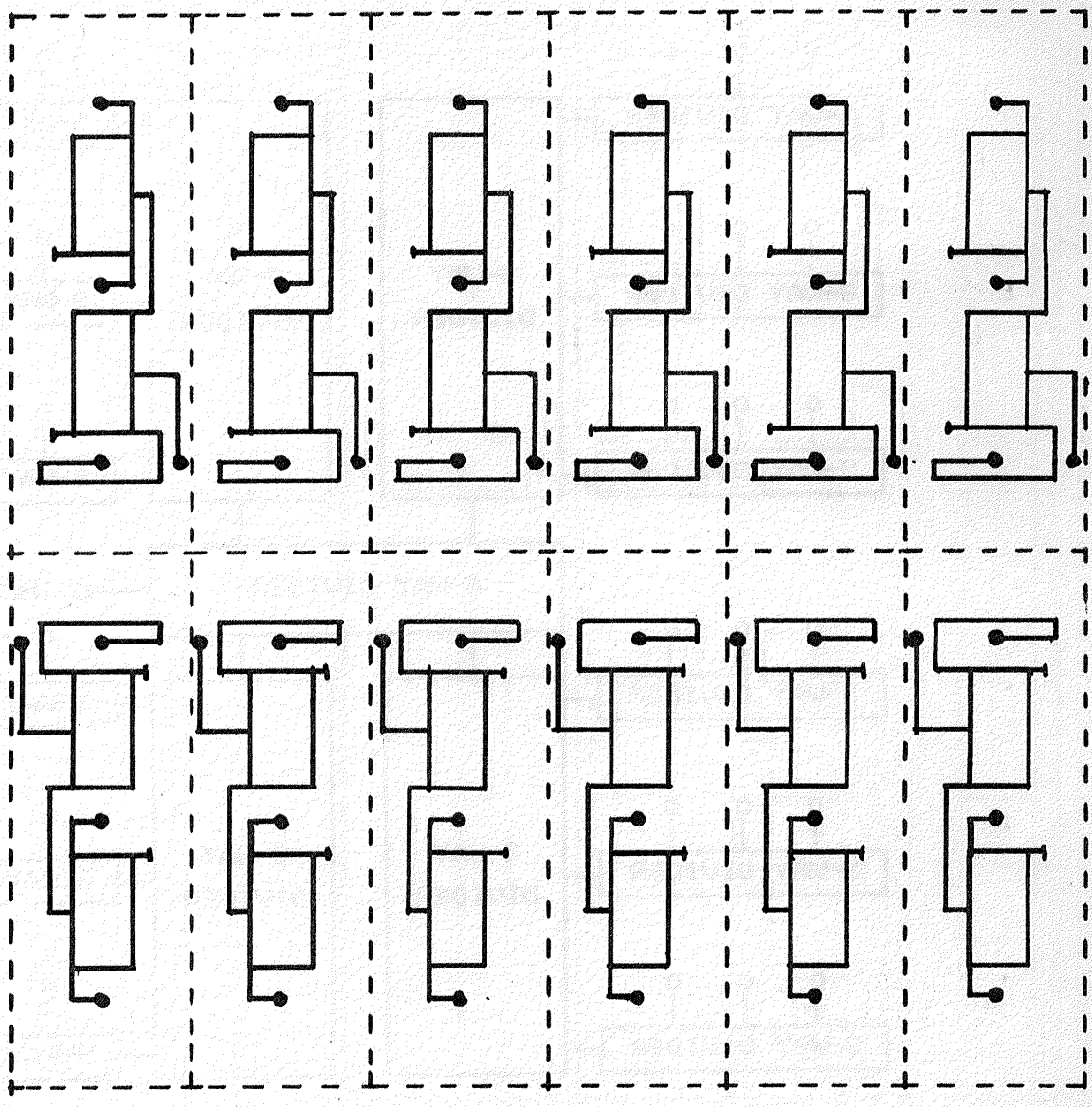

Figure 6. Layout of stripline network for bottom layer of low sidelobe 6X6 array.

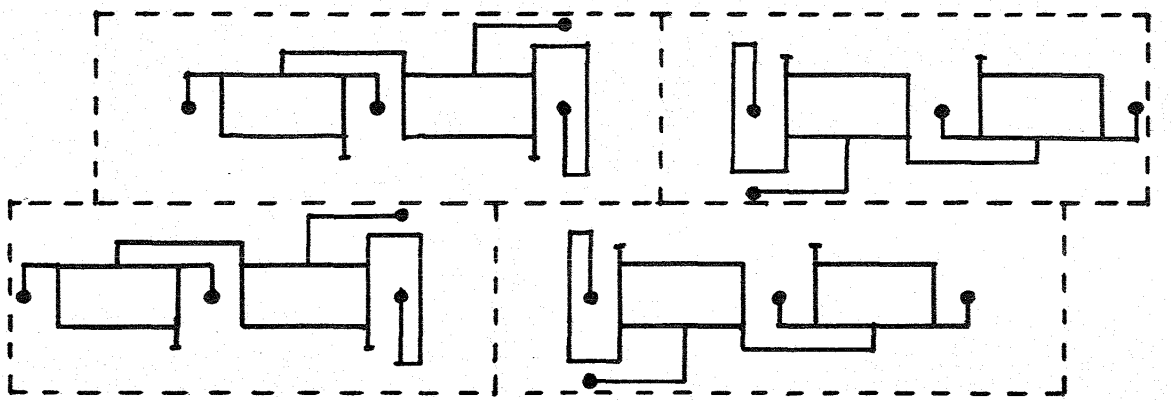

Figure 7. Layout of stripline network for middle layer of low sidelobe 6X6 array.

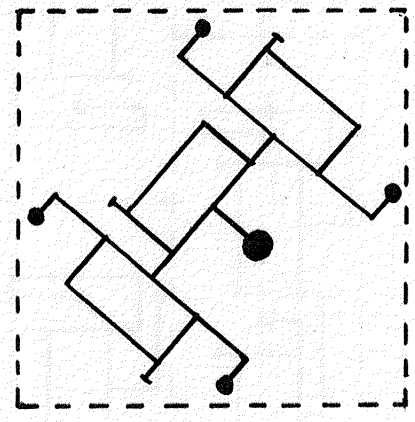

Figure 8. Layout of stripline network for top layer of low sidelobe 6X6 array.

NASA
L-82-5,251

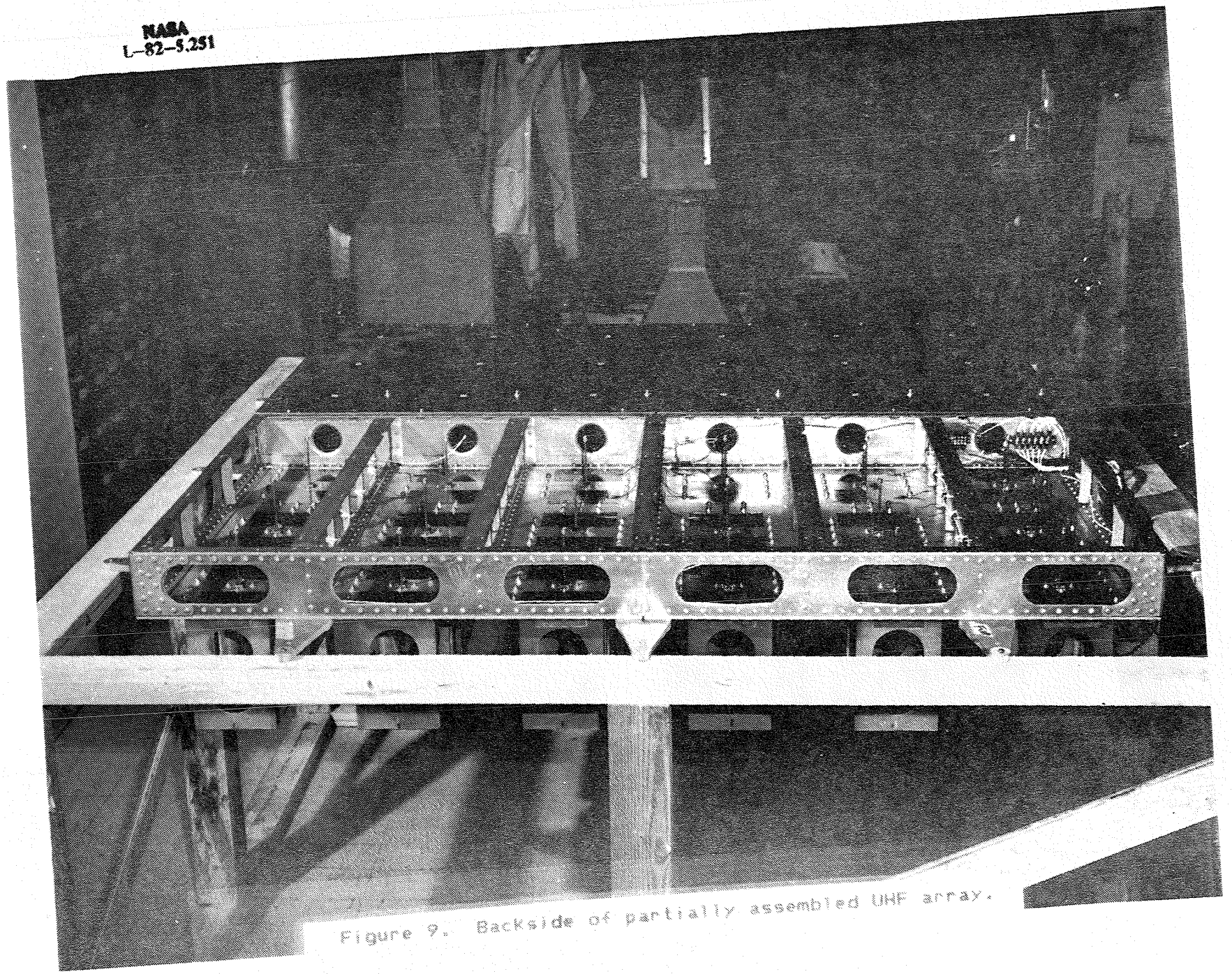

Figure 9. Backside of partially assembled UHF array.

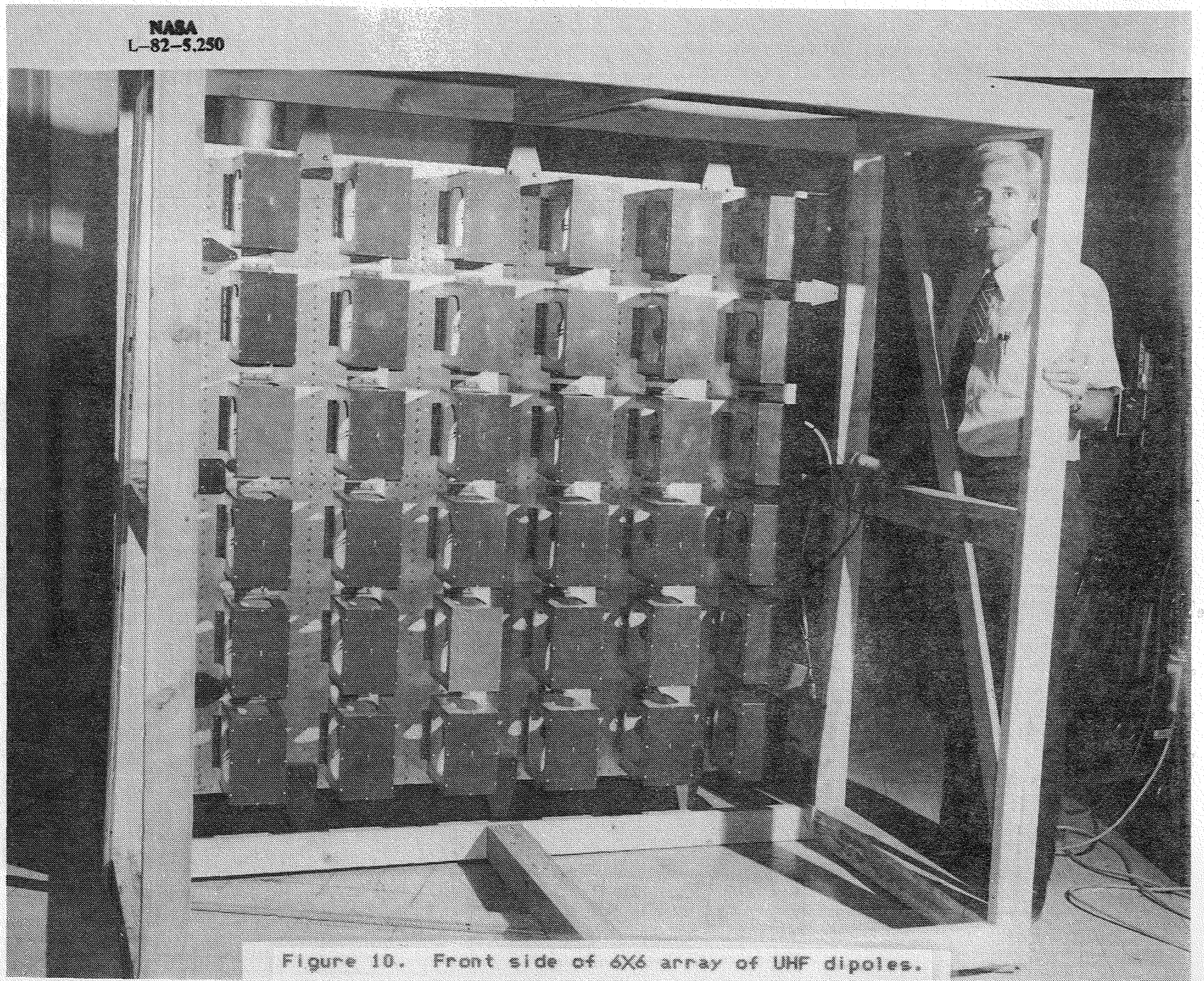

Figure 10. Front side of 6X6 array of UHF dipoles.

NASA
L-82-6,432

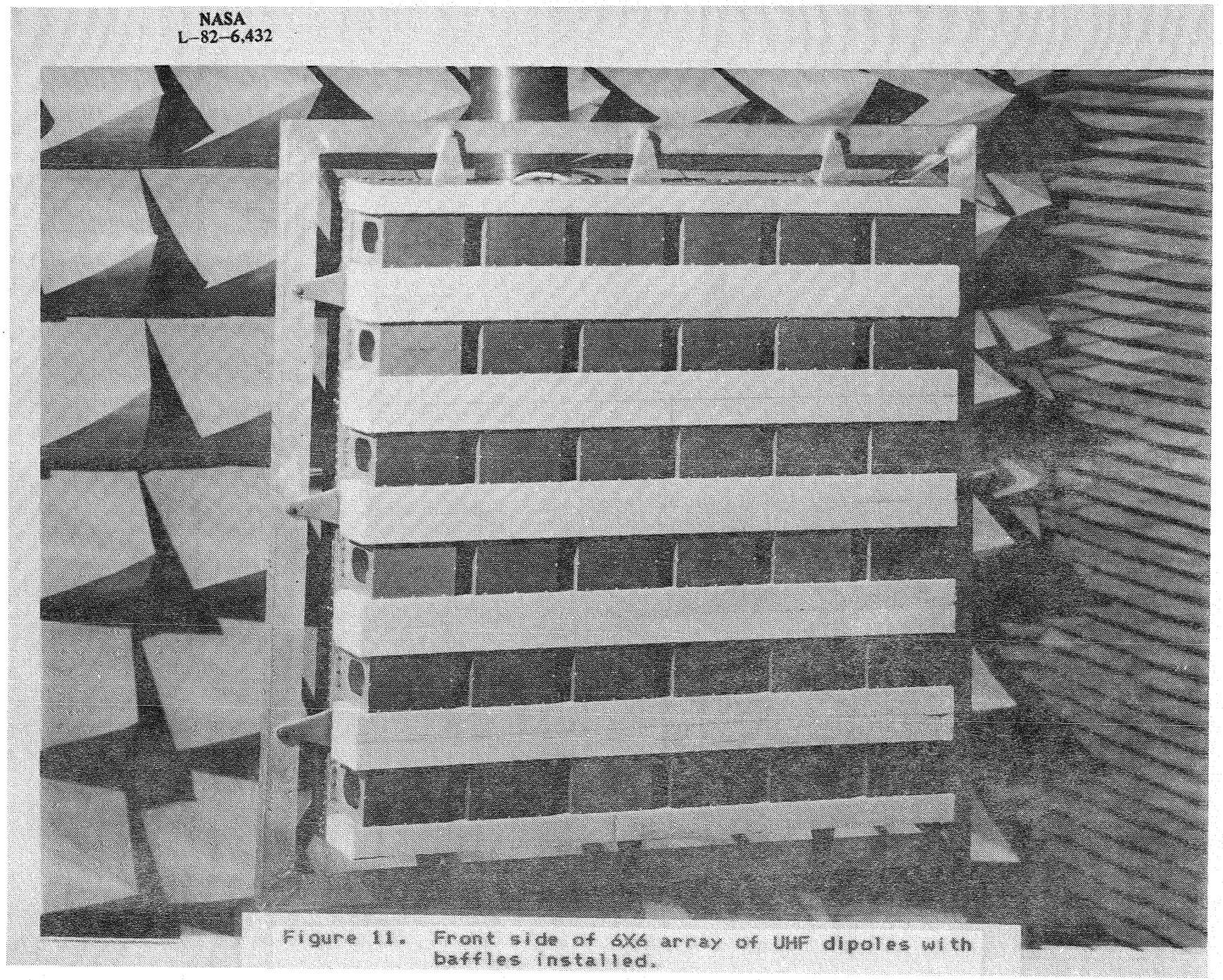

Figure 11. Front side of 6X6 array of UHF dipoles with baffles installed.

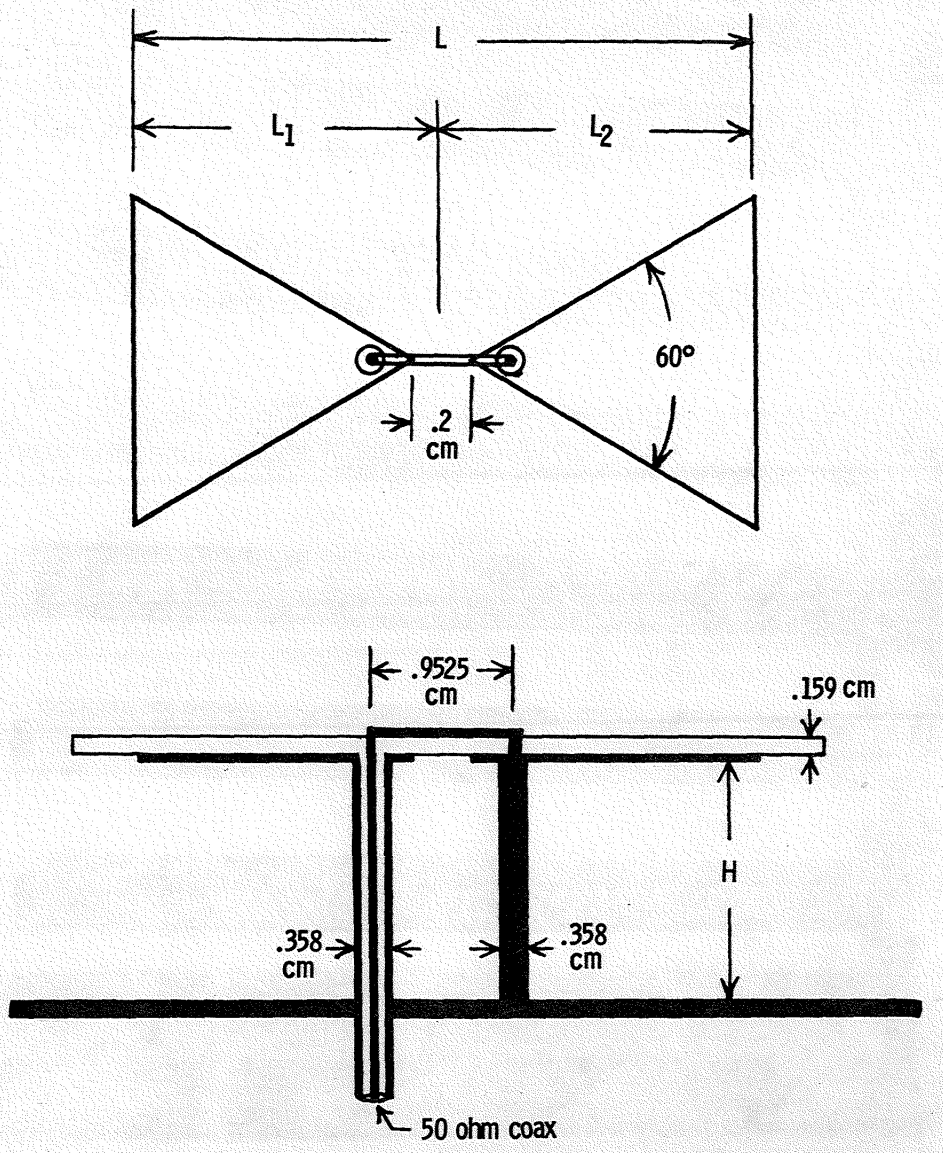

Figure 12. Dimensional drawing of UHF dipole.

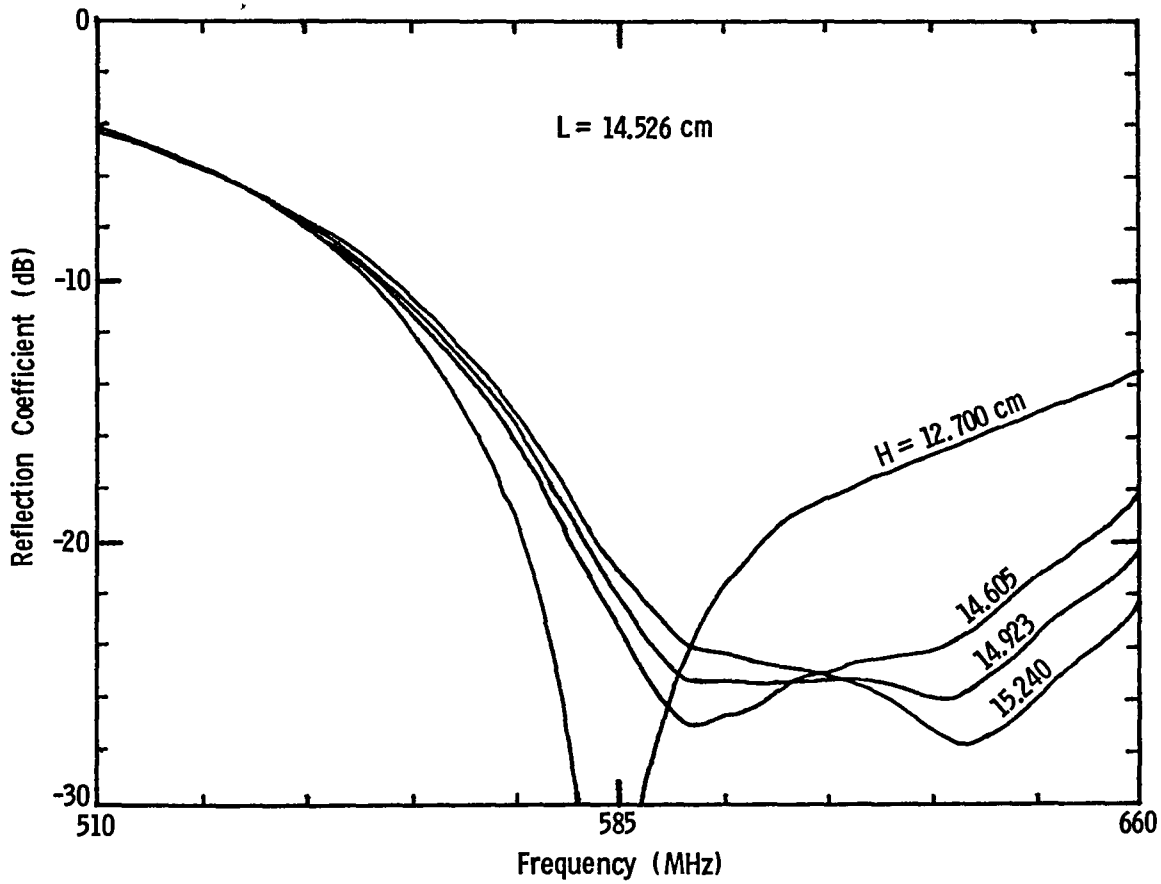

Figure 13. Effect of dipole height upon reflection coefficient.

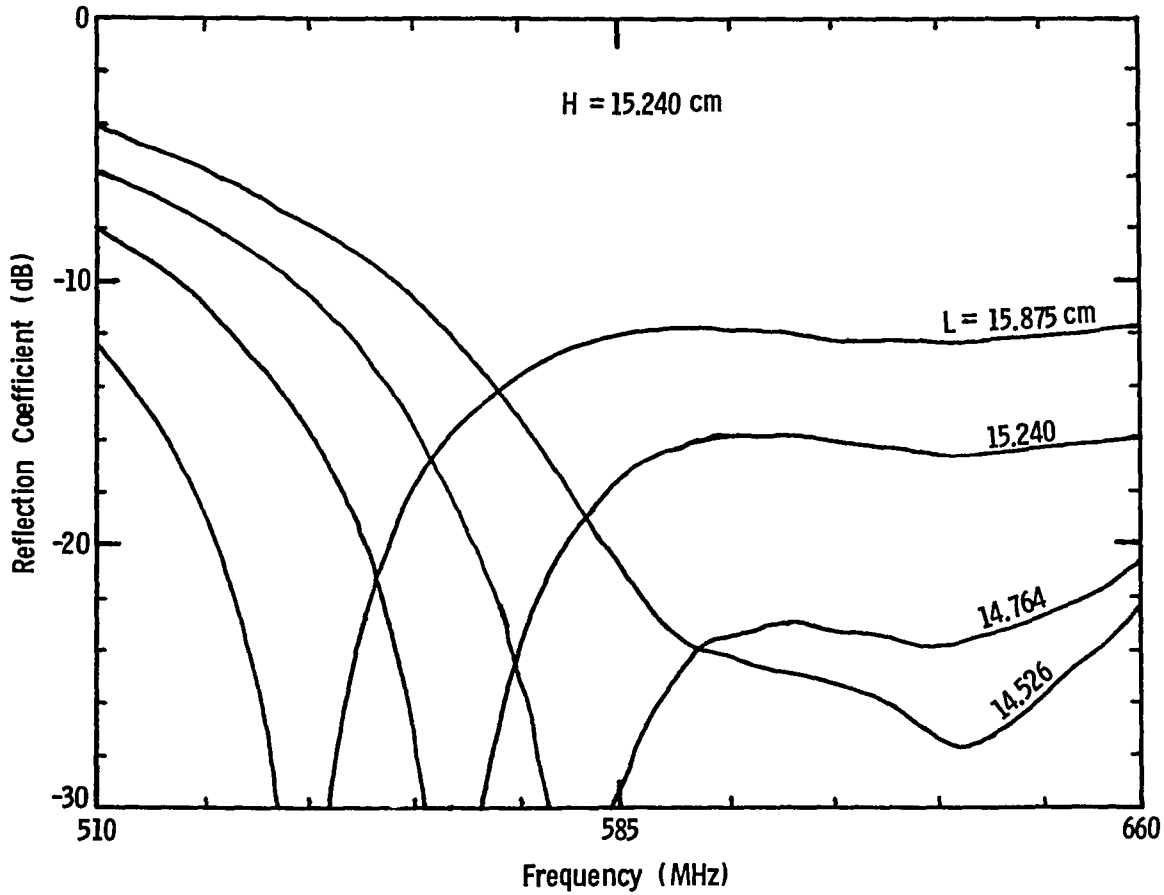

Figure 14. Effect of dipole length upon reflection coefficient.

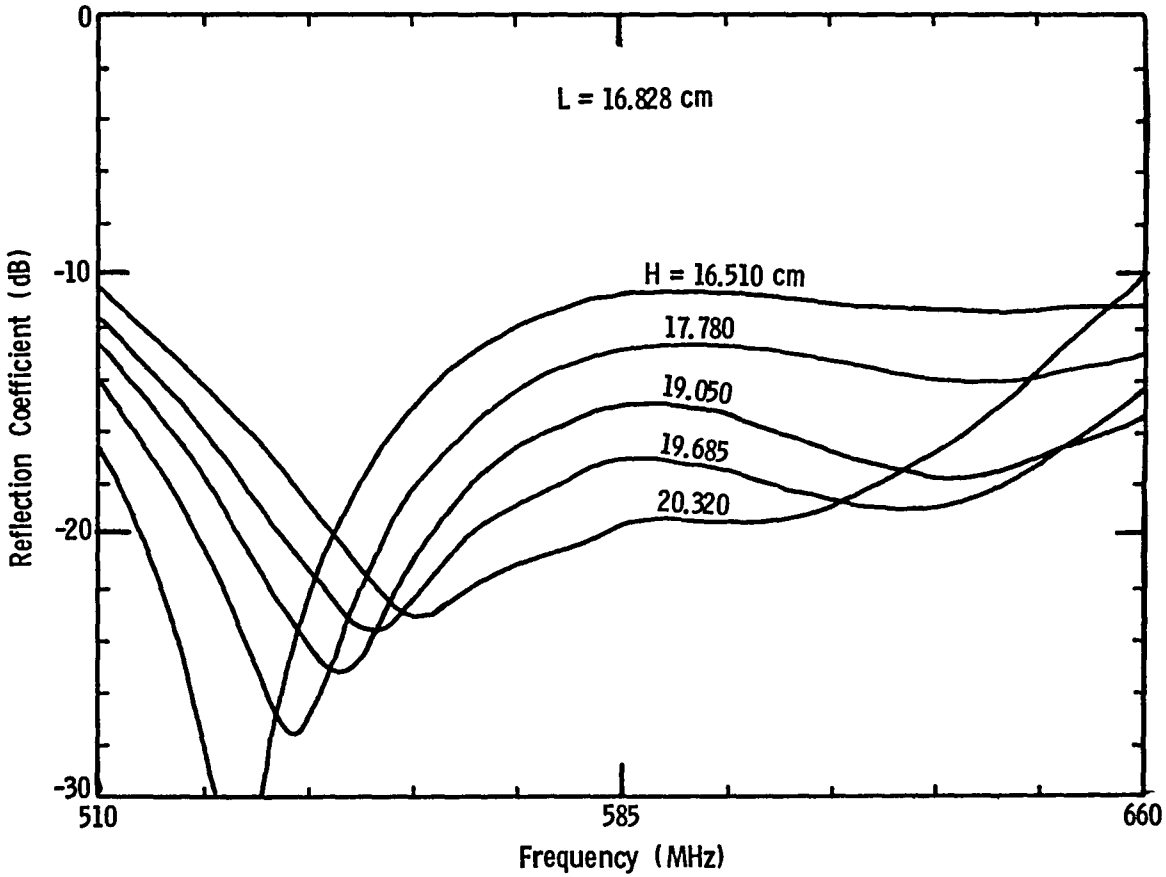

Figure 15. Broad-band optimization of fan-dipole.

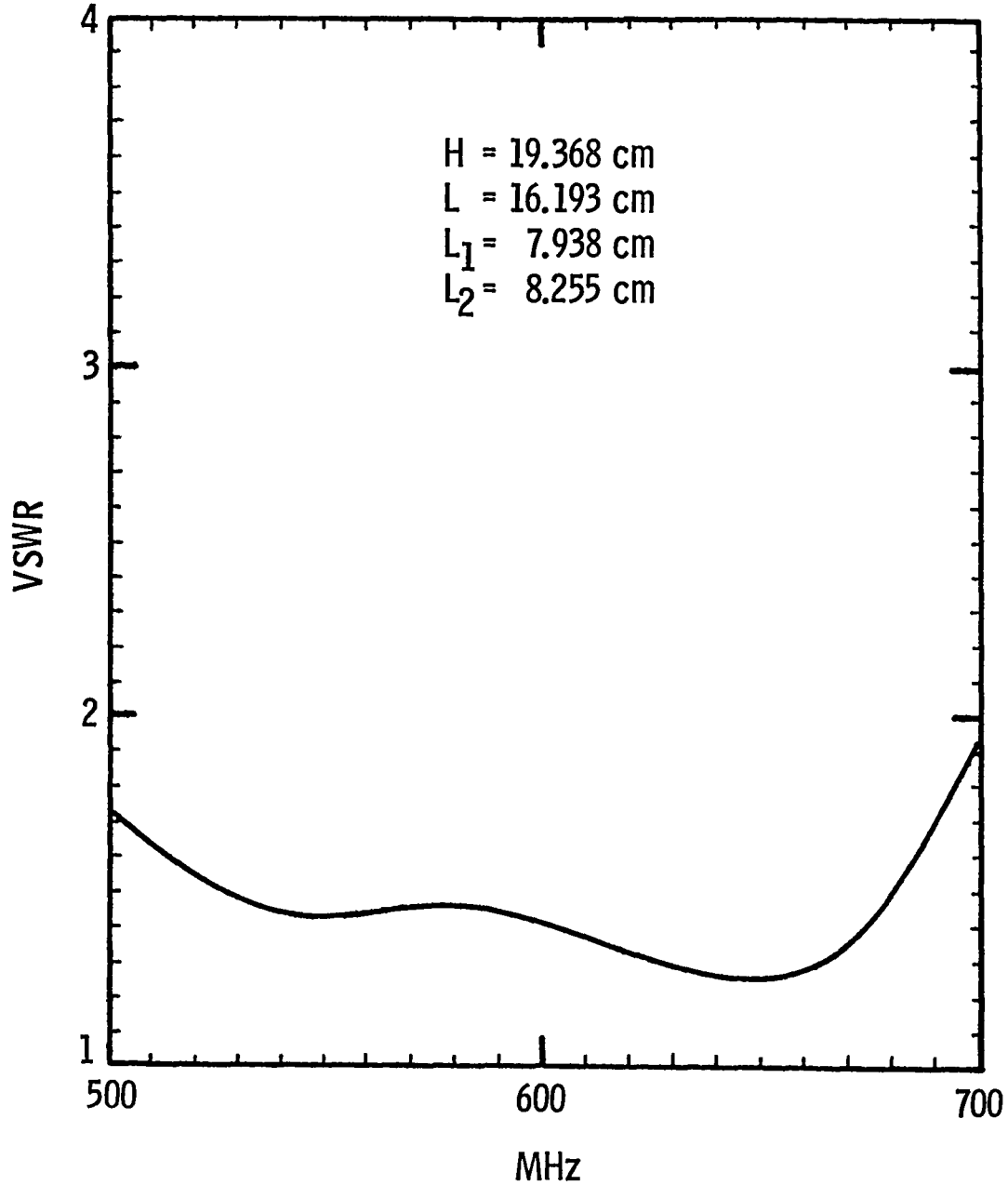

Figure 16. VSWR of broad-band optimized dipole.

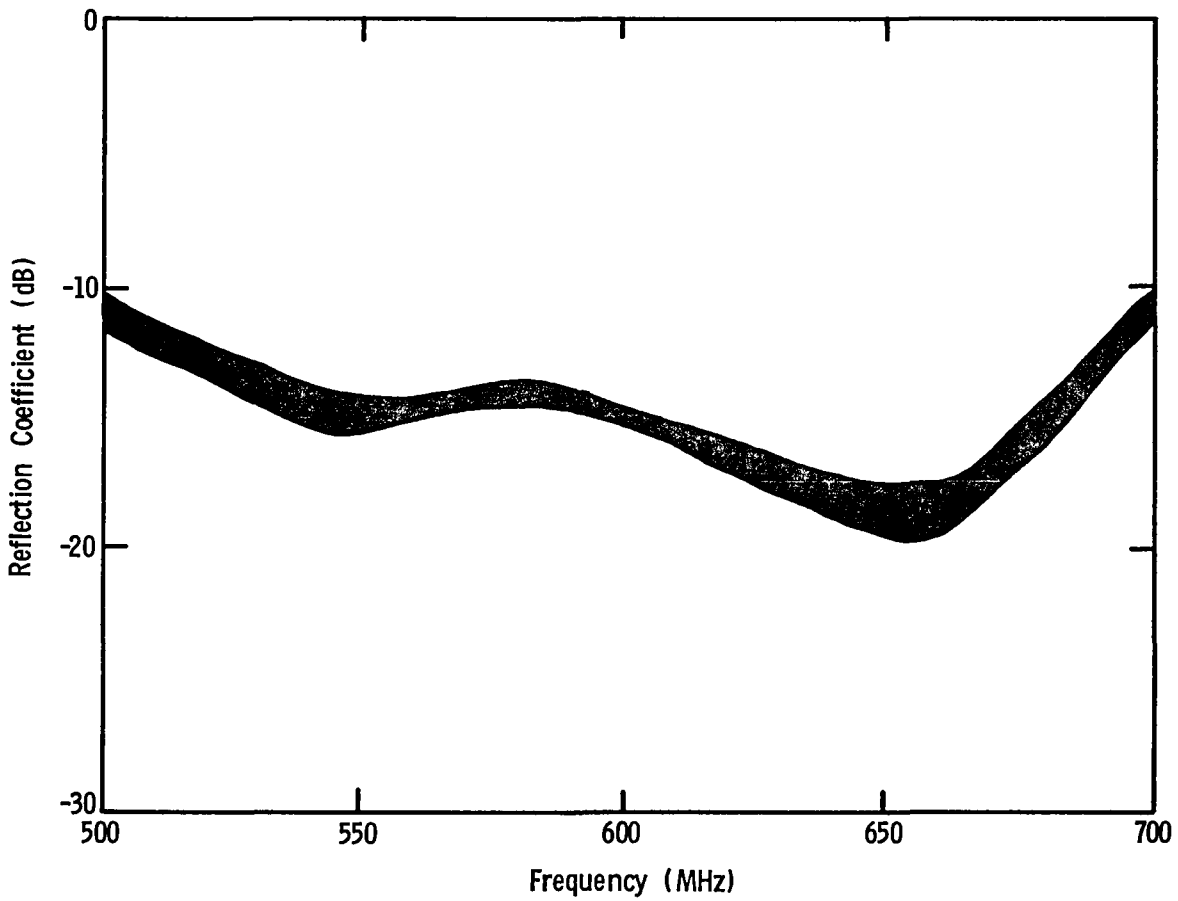

Figure 17. Measured reflection coefficient for all 36 UHF fan-dipoles.

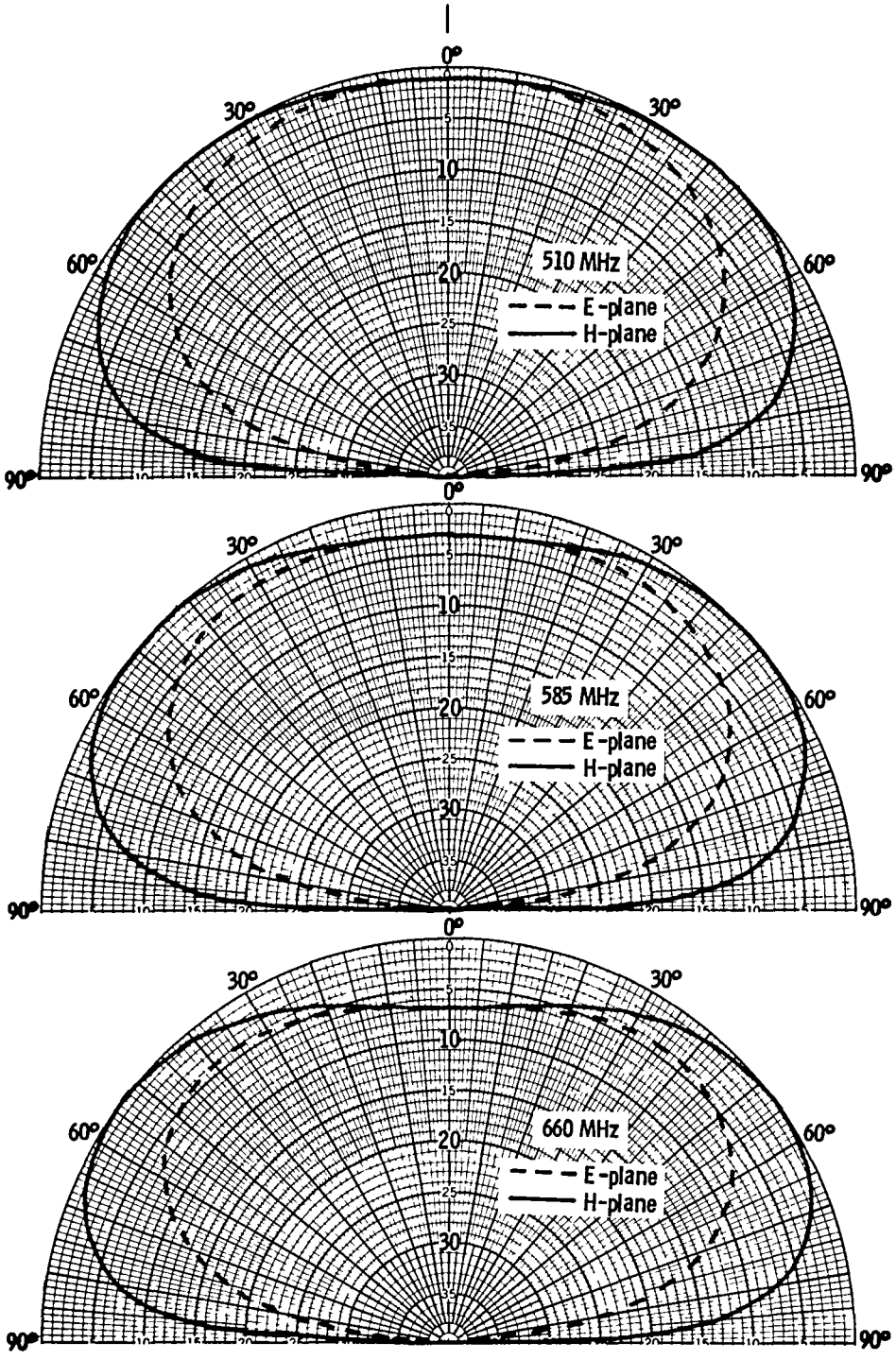

Figure 18. Calculated radiation patterns for linear dipole over infinite ground plane.

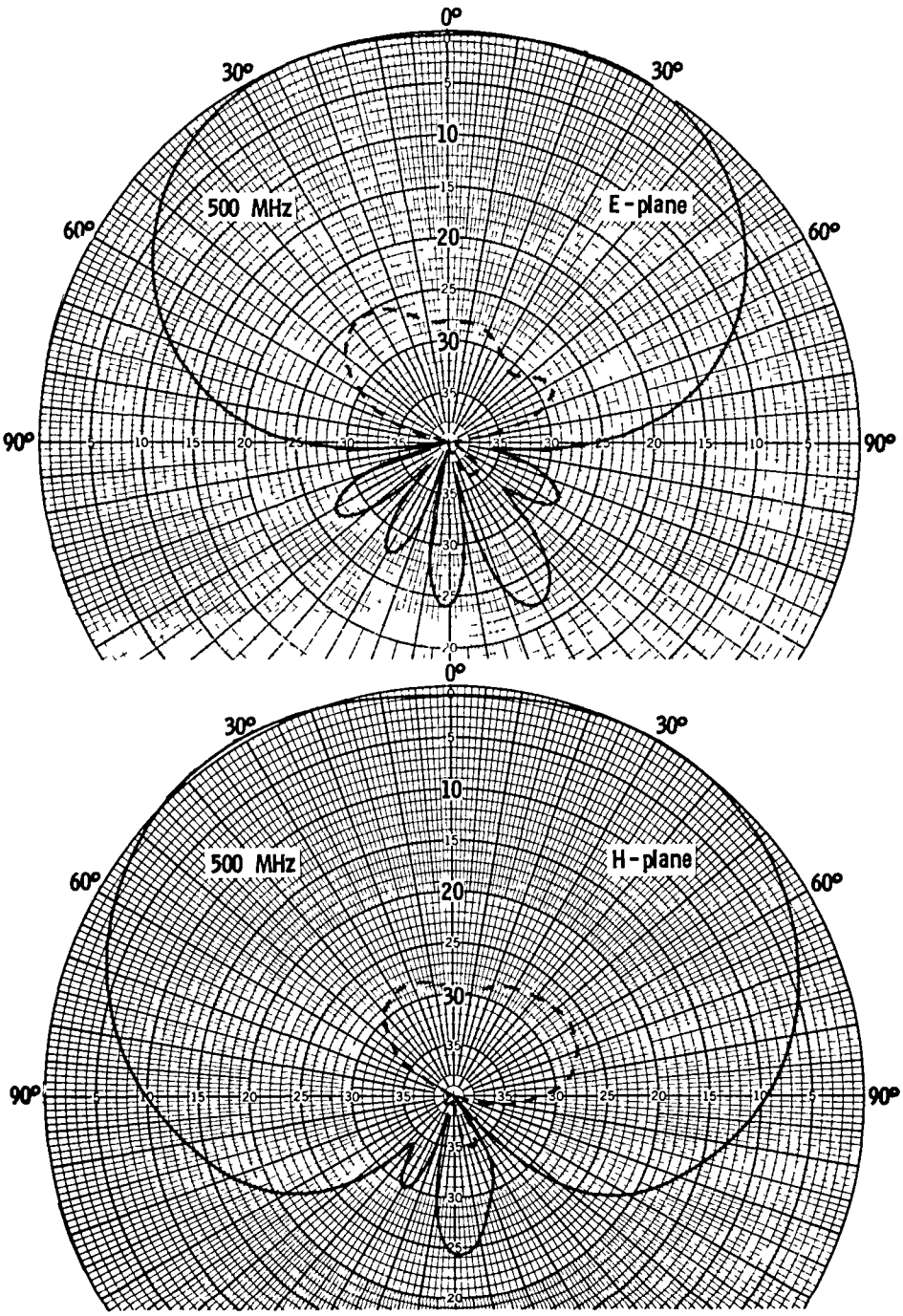

Figure 19. Measured radiation patterns for fan-dipole over 122cm X 122cm ground plane at 500 MHz.

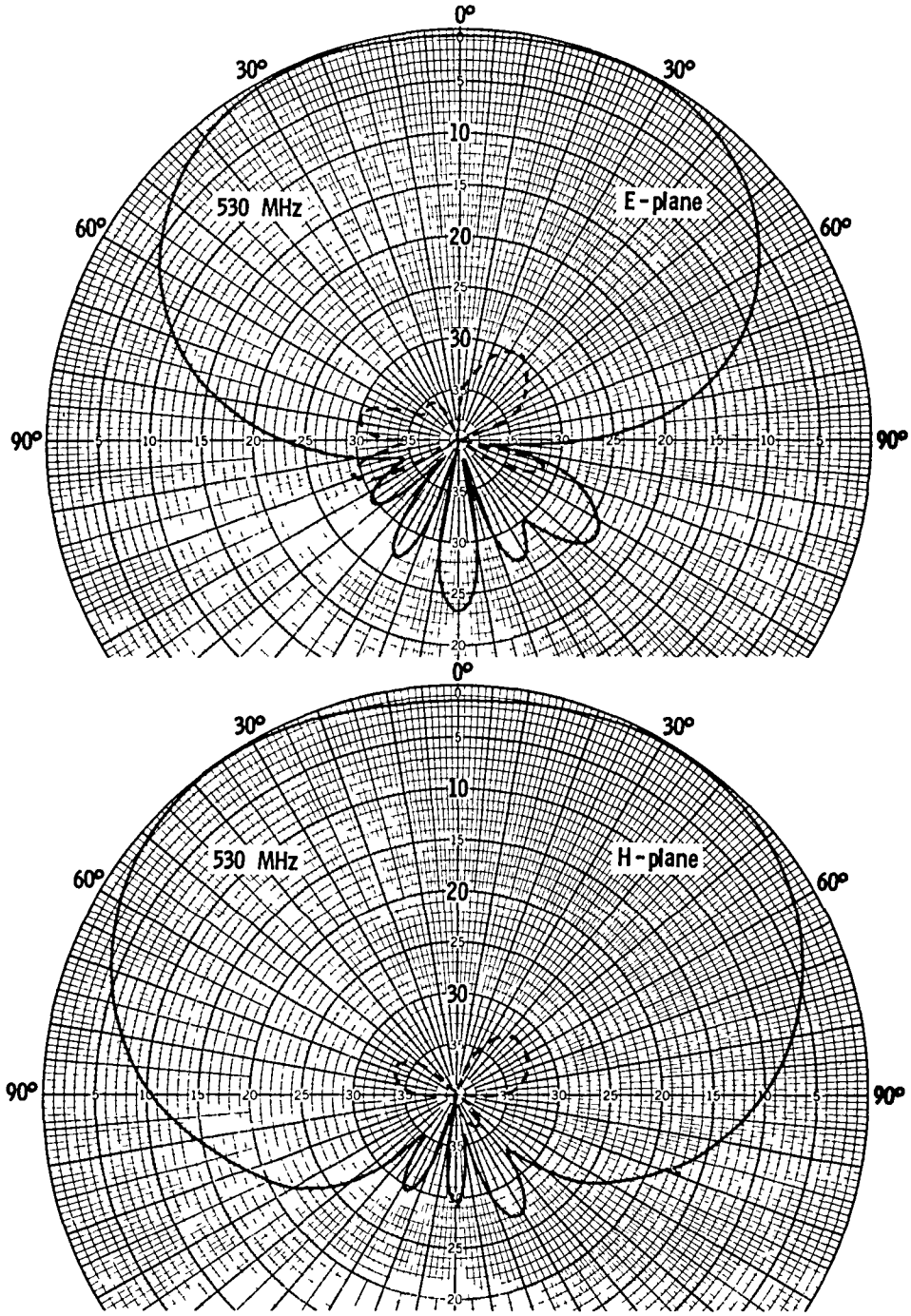

Figure 20. Measured radiation patterns for fan-dipole over 122cm X 122cm ground plane at 530 MHz.

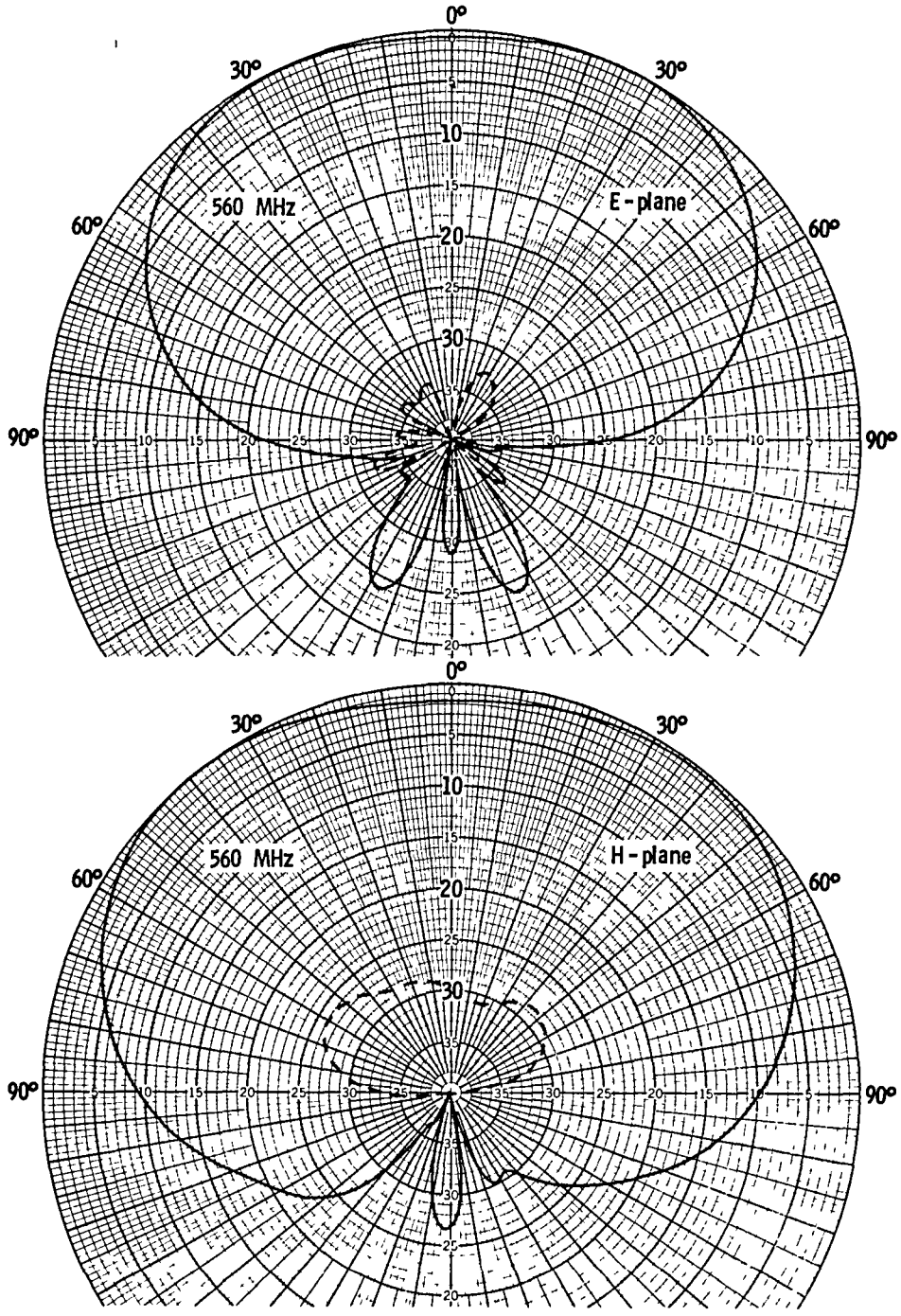

Figure 21. Measured radiation patterns for fan-dipole over 122cm X 122cm ground plane at 560 MHz.

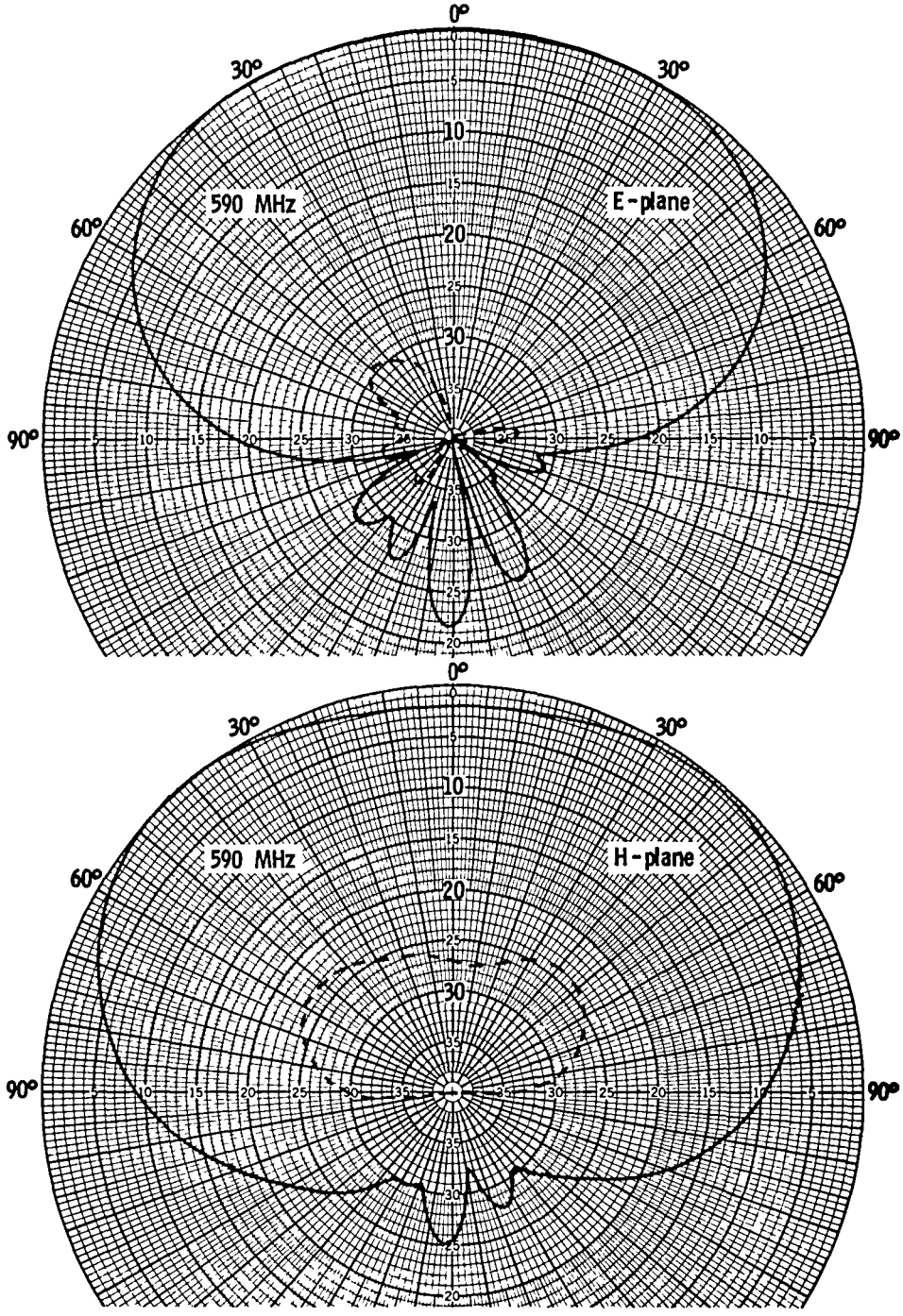

Figure 22. Measured radiation patterns for fan-dipole over 122cm X 122cm ground plane at 590 MHz.

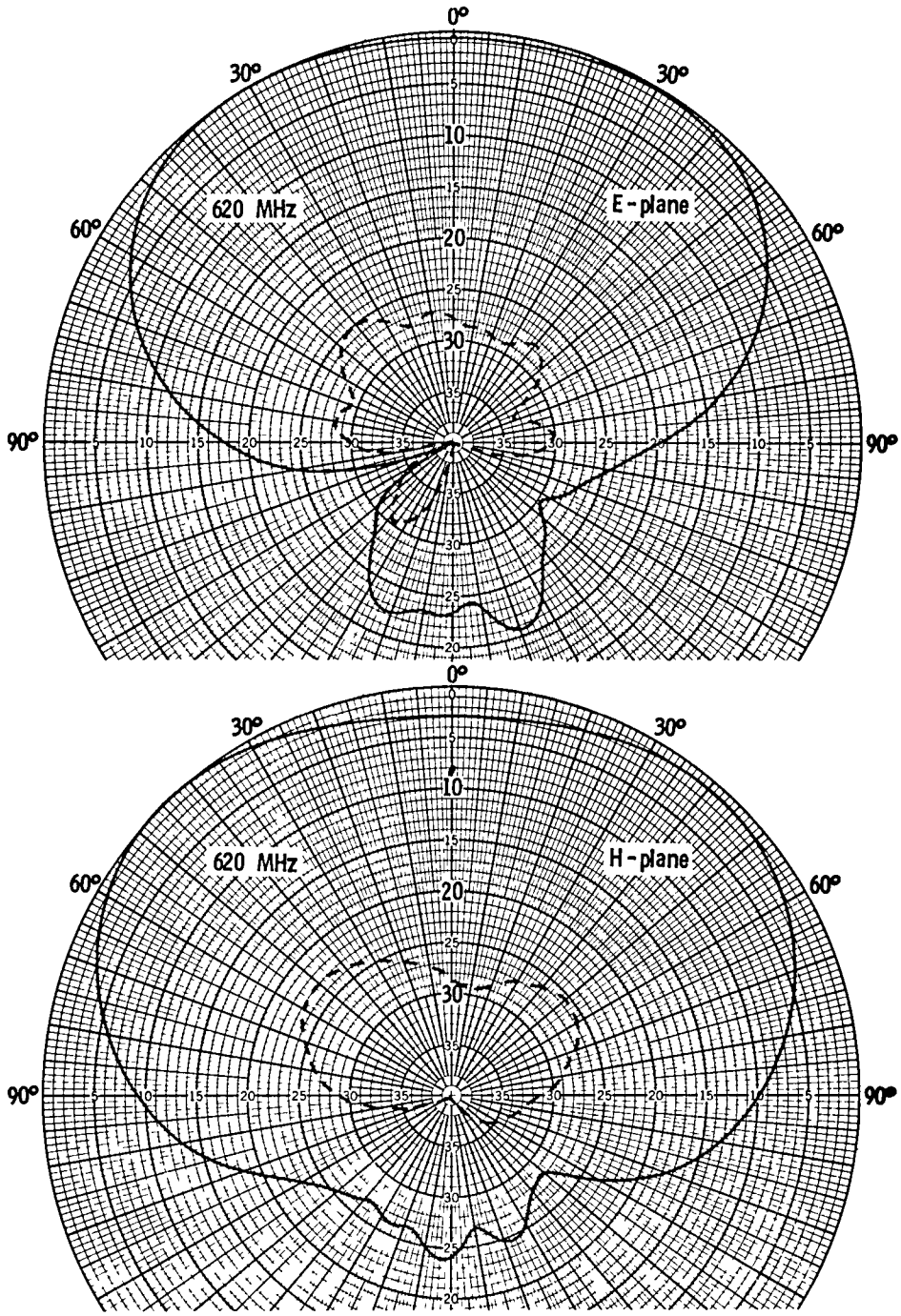

Figure 23. Measured radiation patterns for fan-dipole over 122cm X 122cm ground plane at 620 MHz.

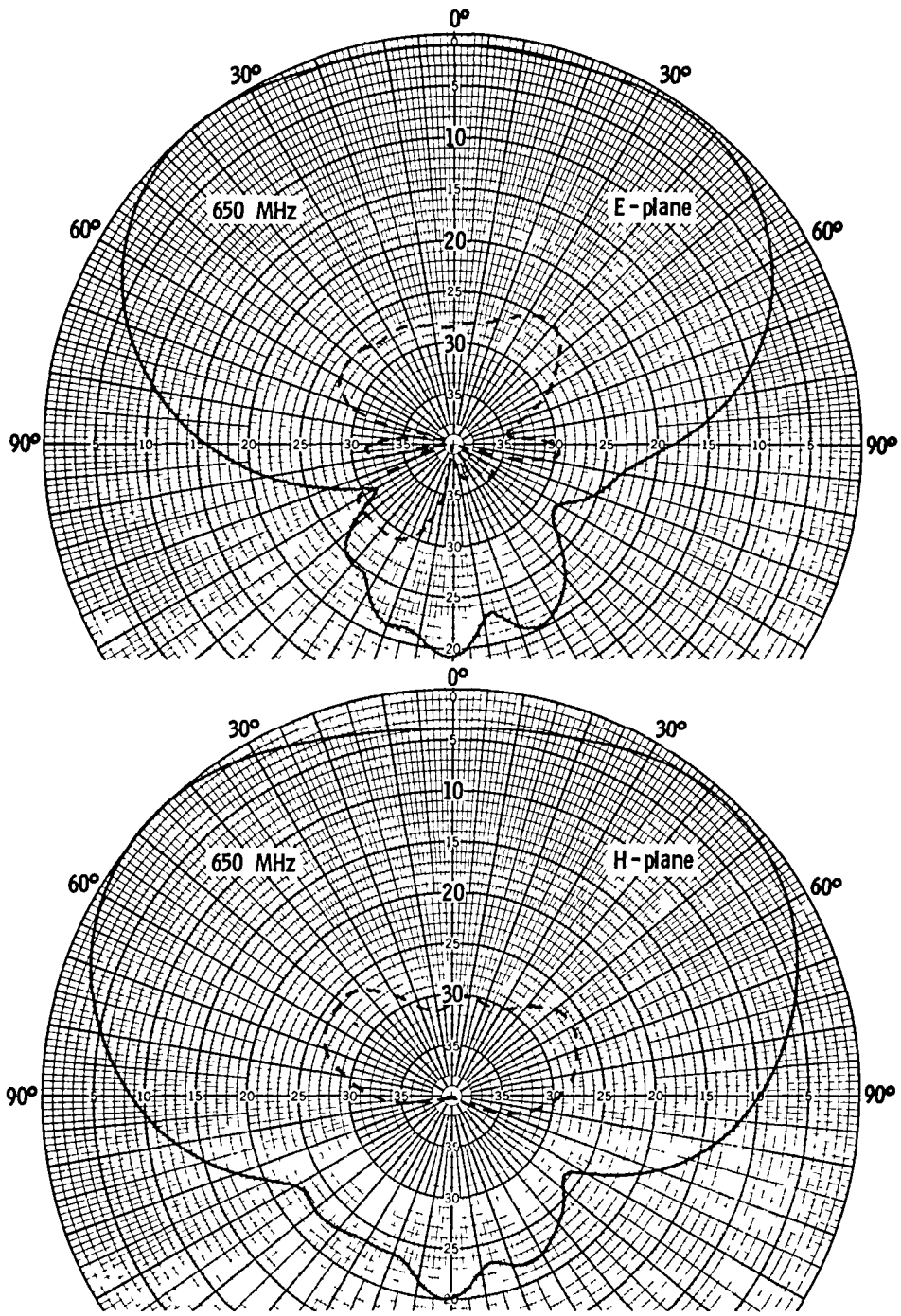

Figure 24. Measured radiation patterns for fan-dipole over 122cm X 122cm ground plane at 650 MHz.

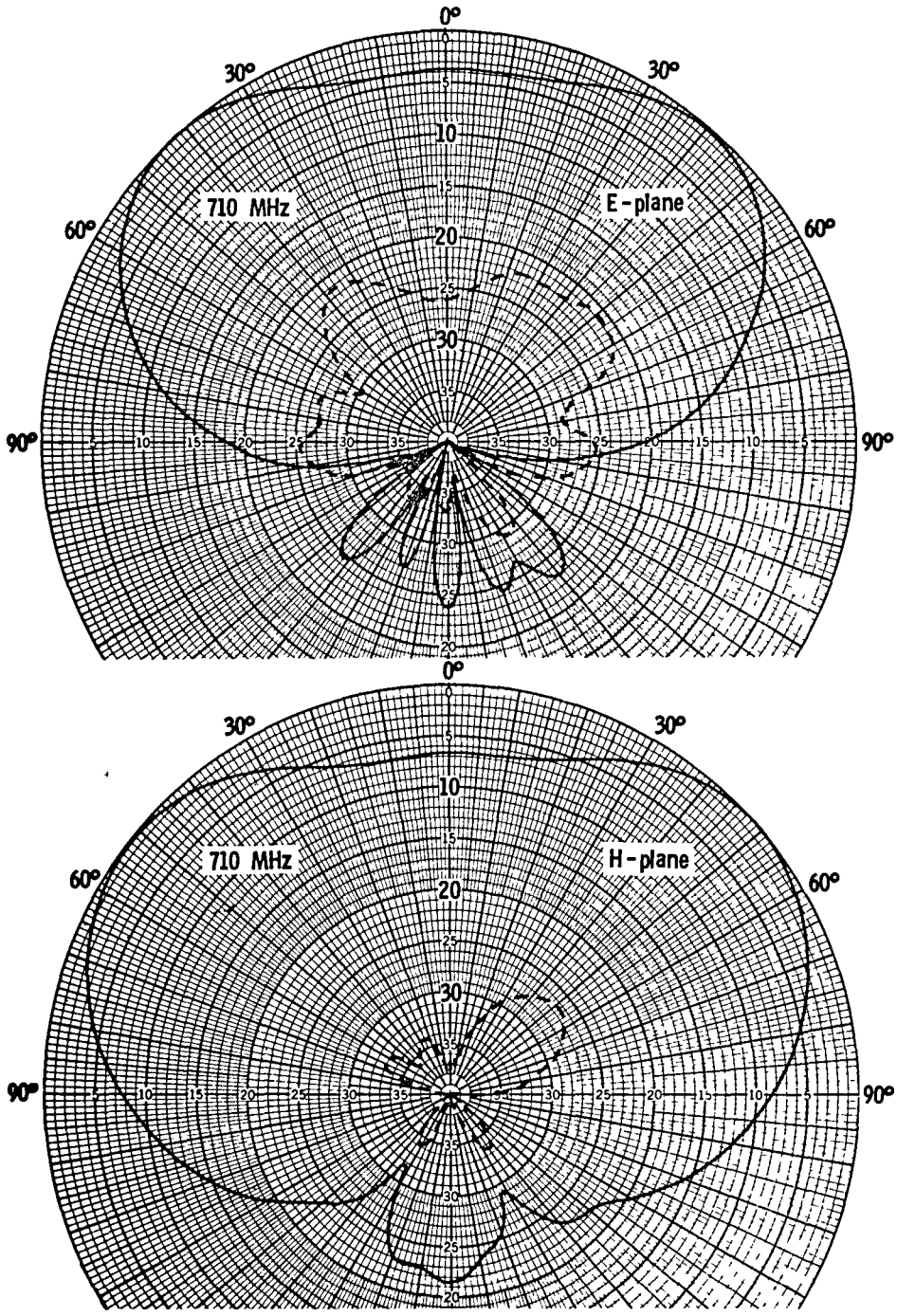

Figure 25. Measured radiation patterns for fan-dipole over 122cm X 122cm ground plane at 710 MHz.

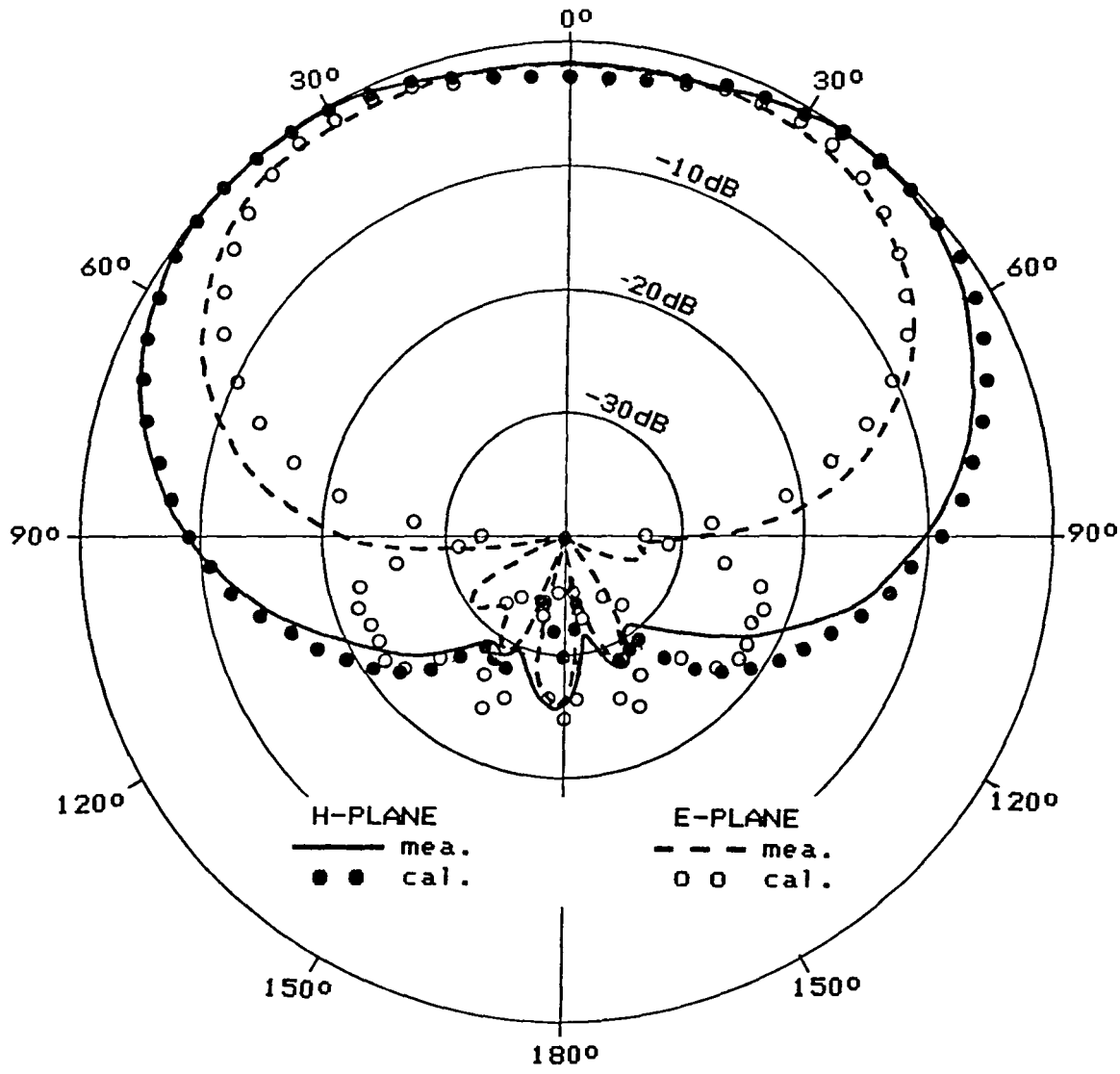

Figure 26. Calculated radiation patterns for linear dipole over 122cm X 122cm ground plane at 590 MHz.

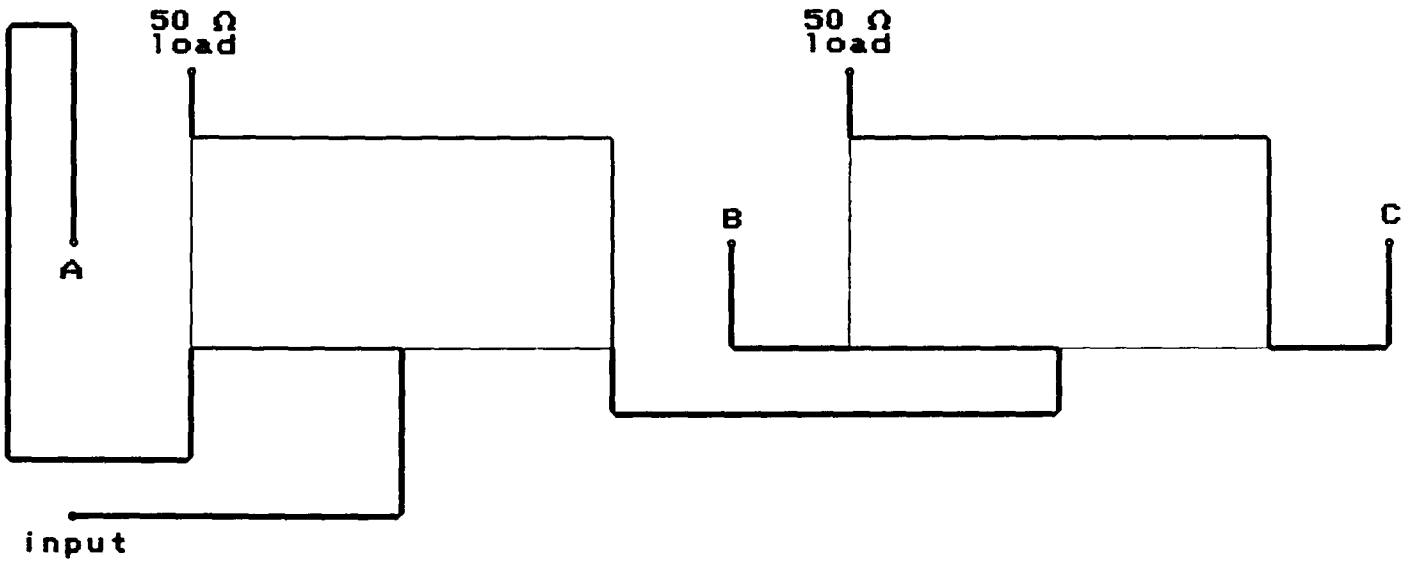

Figure 27. Stripline circuit for 3-way power divider to obtain one-sided cosine distribution.

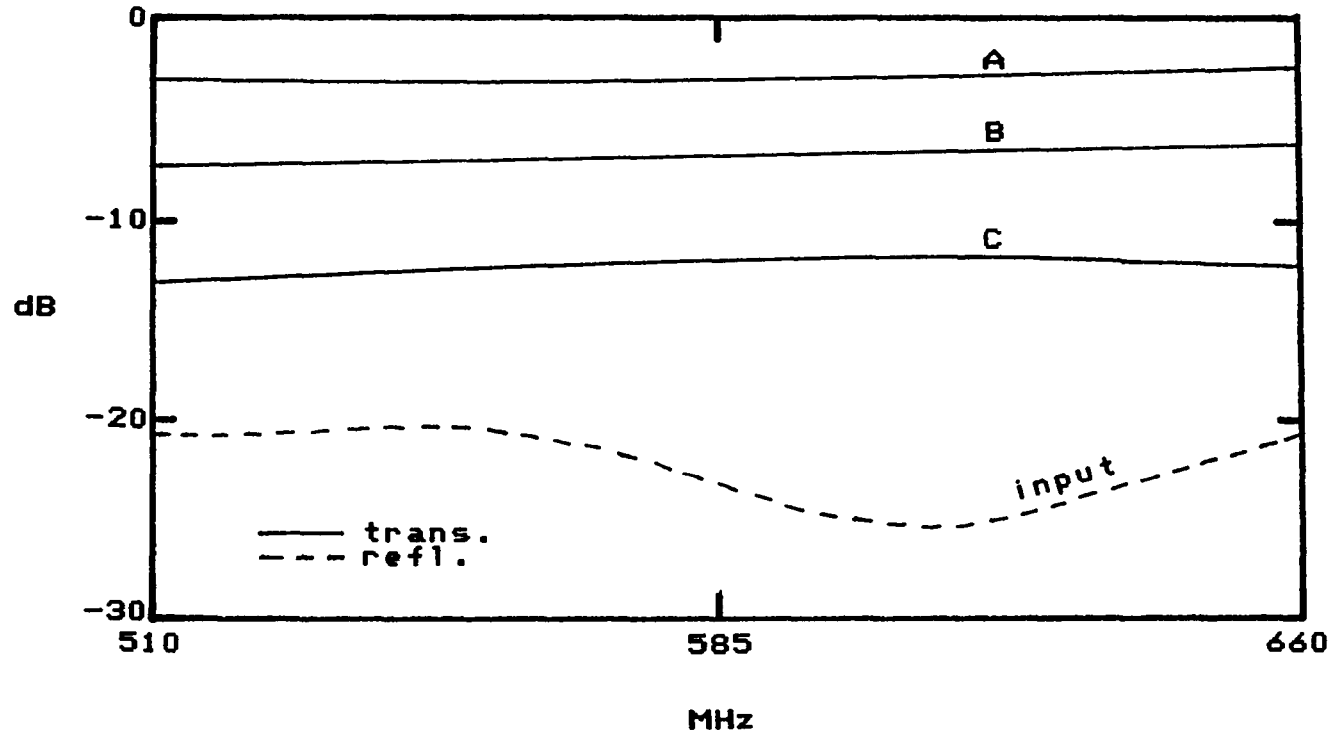

Figure 28. Measured reflection and transmission coefficients for 3-way power divider.

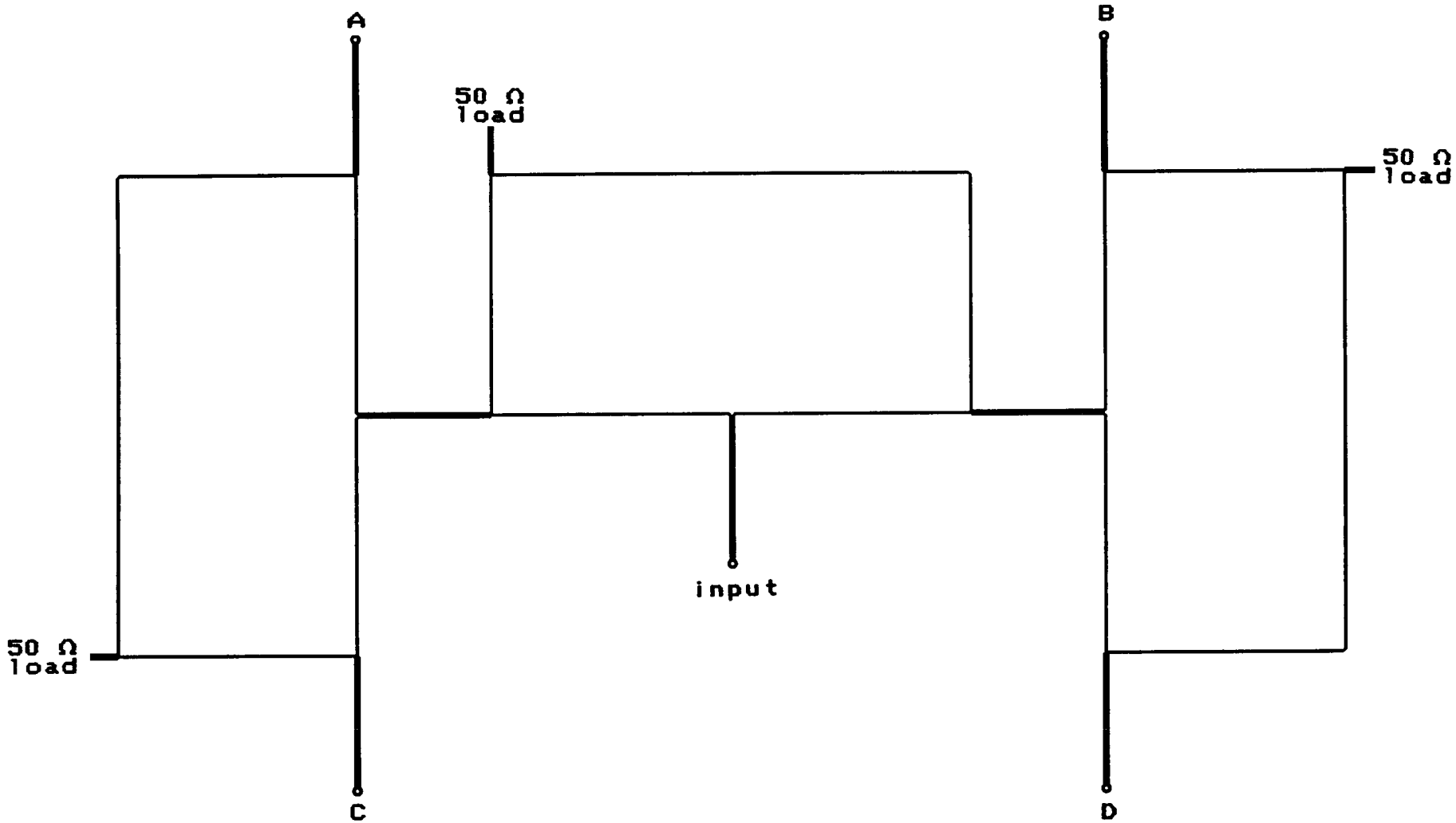

Figure 29. Stripline circuit for 4-way equal-split power divider.

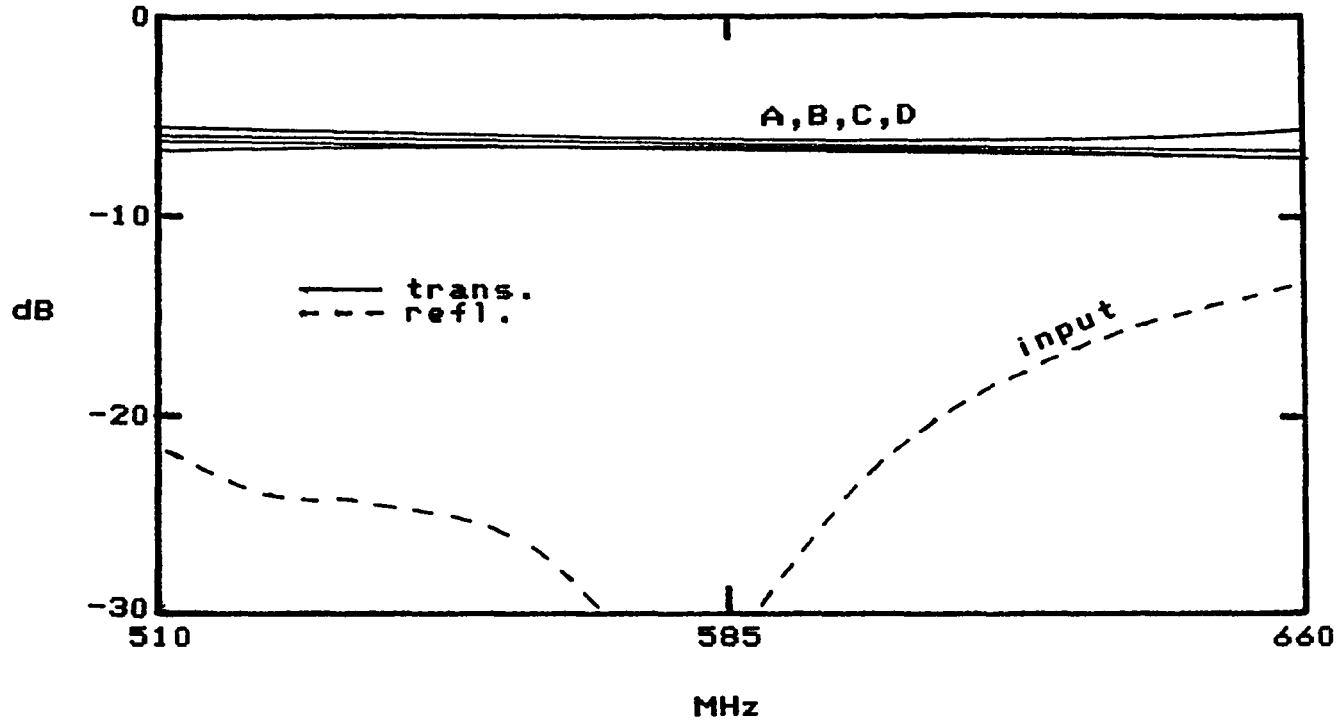

Figure 30. Measured reflection and transmission coefficients for 4-way equal-split power divider.

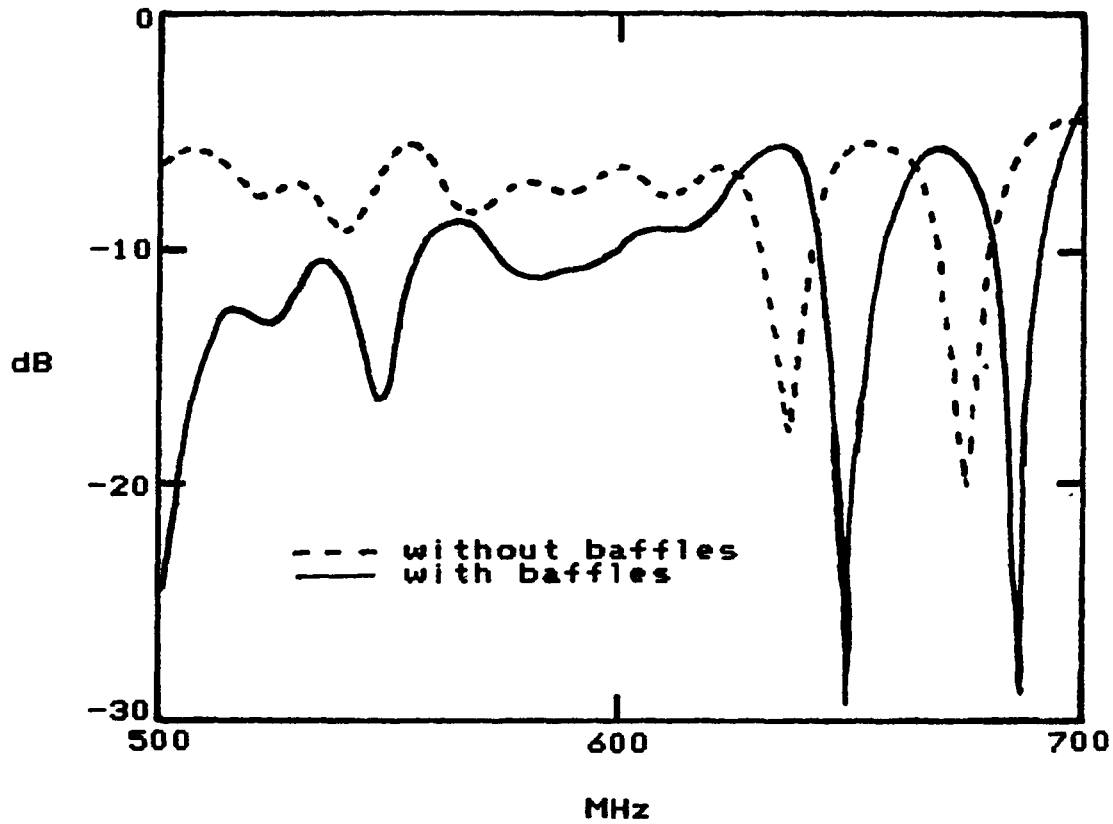

Figure 31. Measured reflection coefficient for 6X6 array with low-sidelobe feed distribution network.

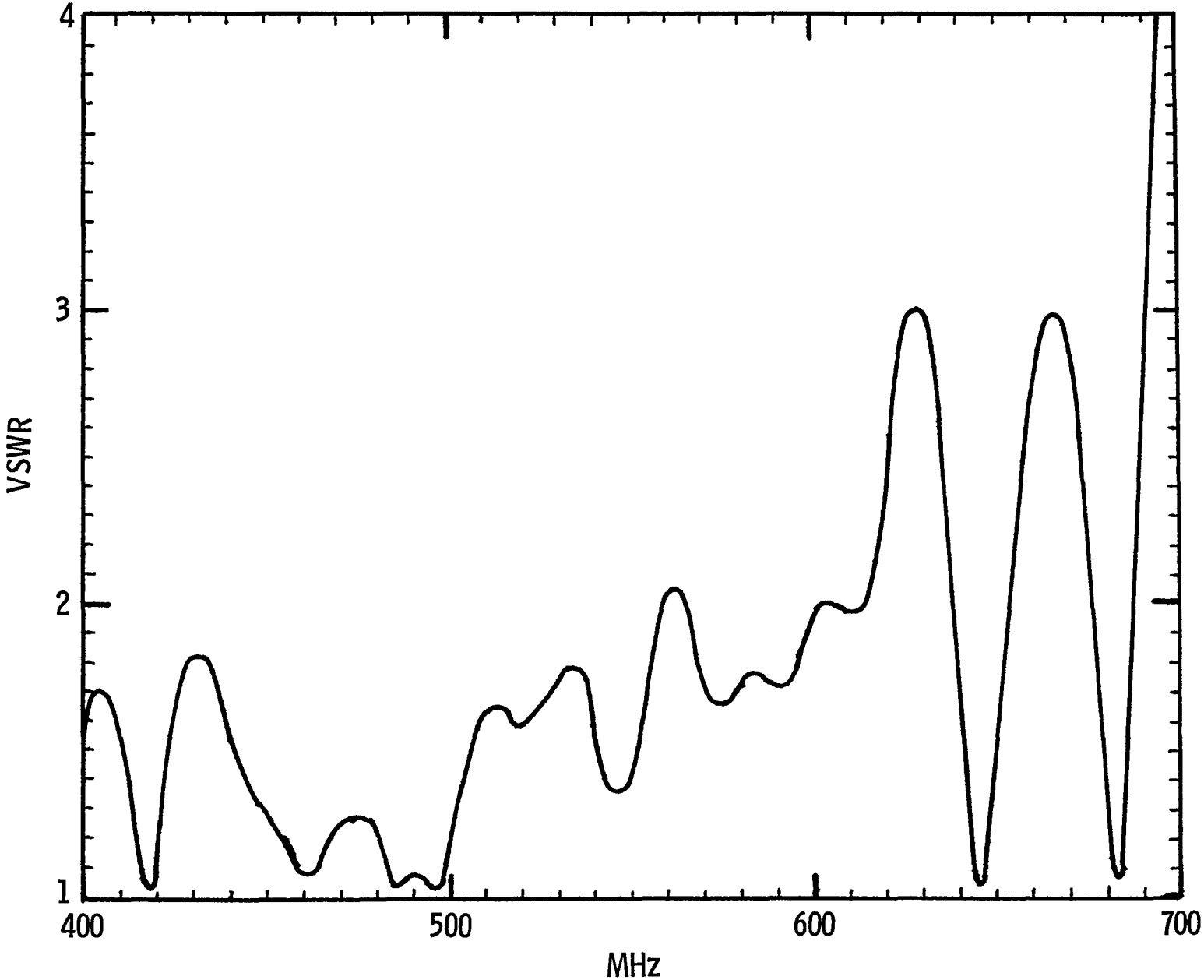

Figure 32. VSWR for final antenna design.

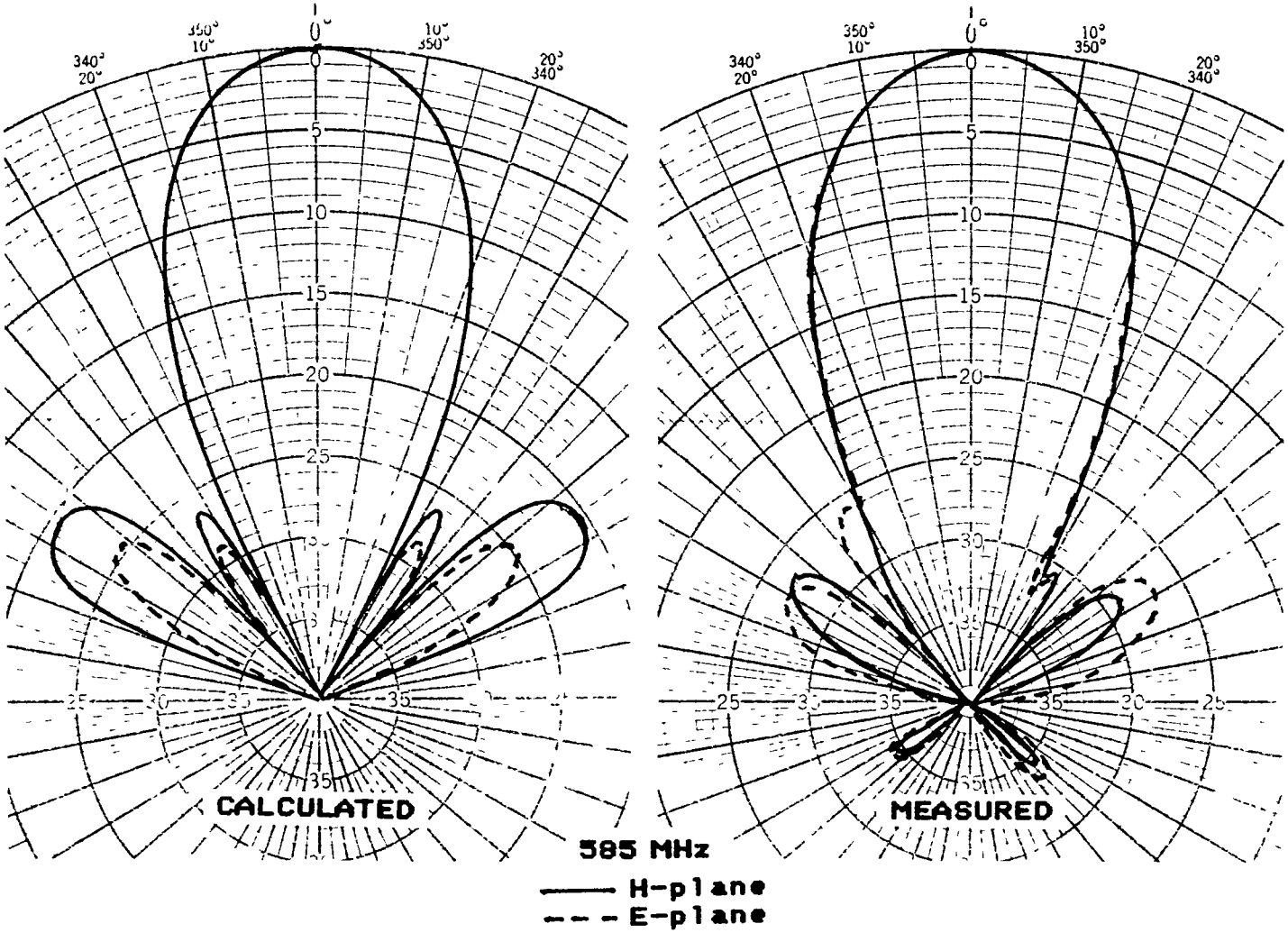

Figure 33. Comparision of measured radiation patterns for fan-dipole array with calculated radiation patterns for array of linear dipoles over infinite ground plane.

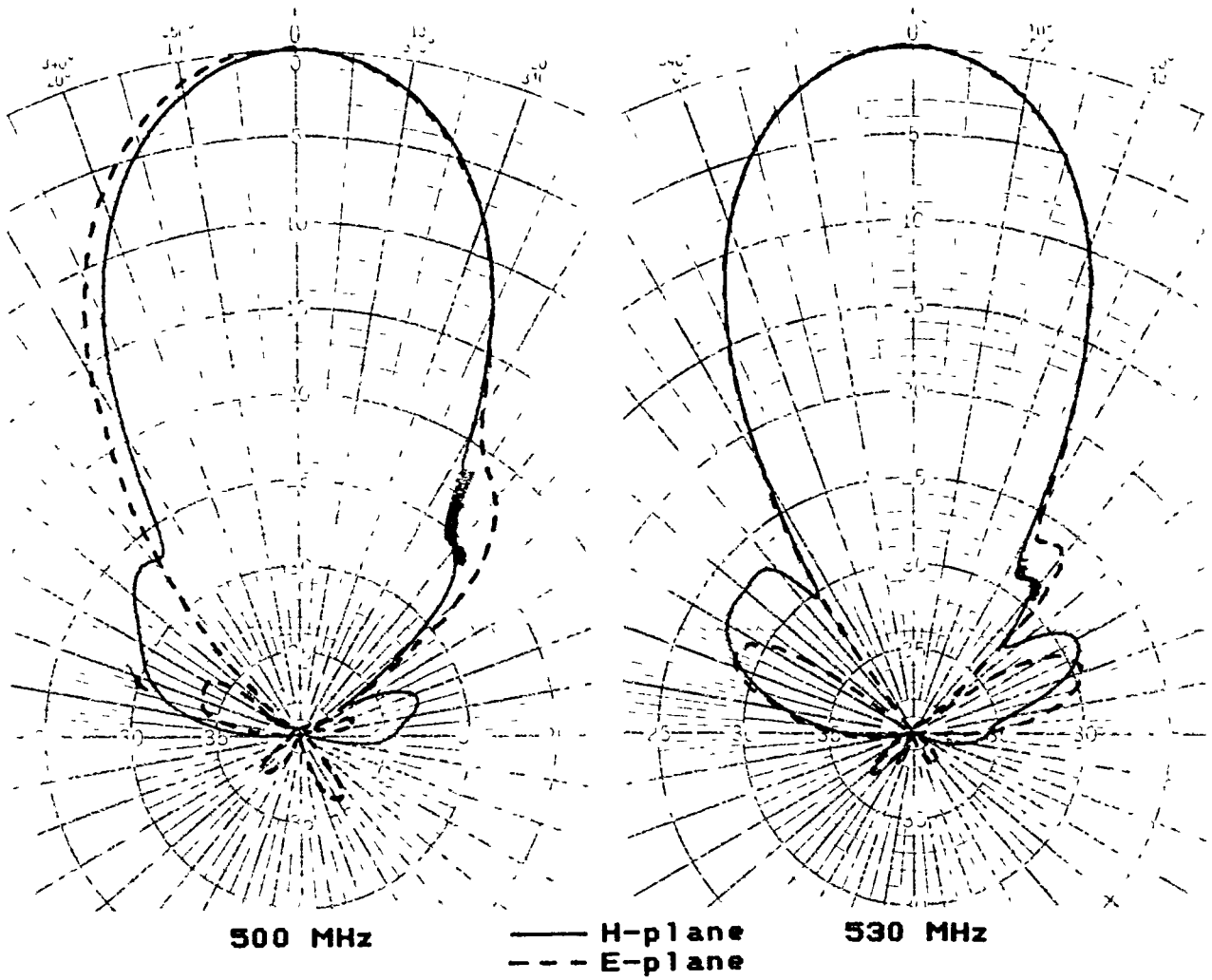

Figure 34. Measured radiation patterns for final UHF antenna array (500 MHz and 530 MHz).

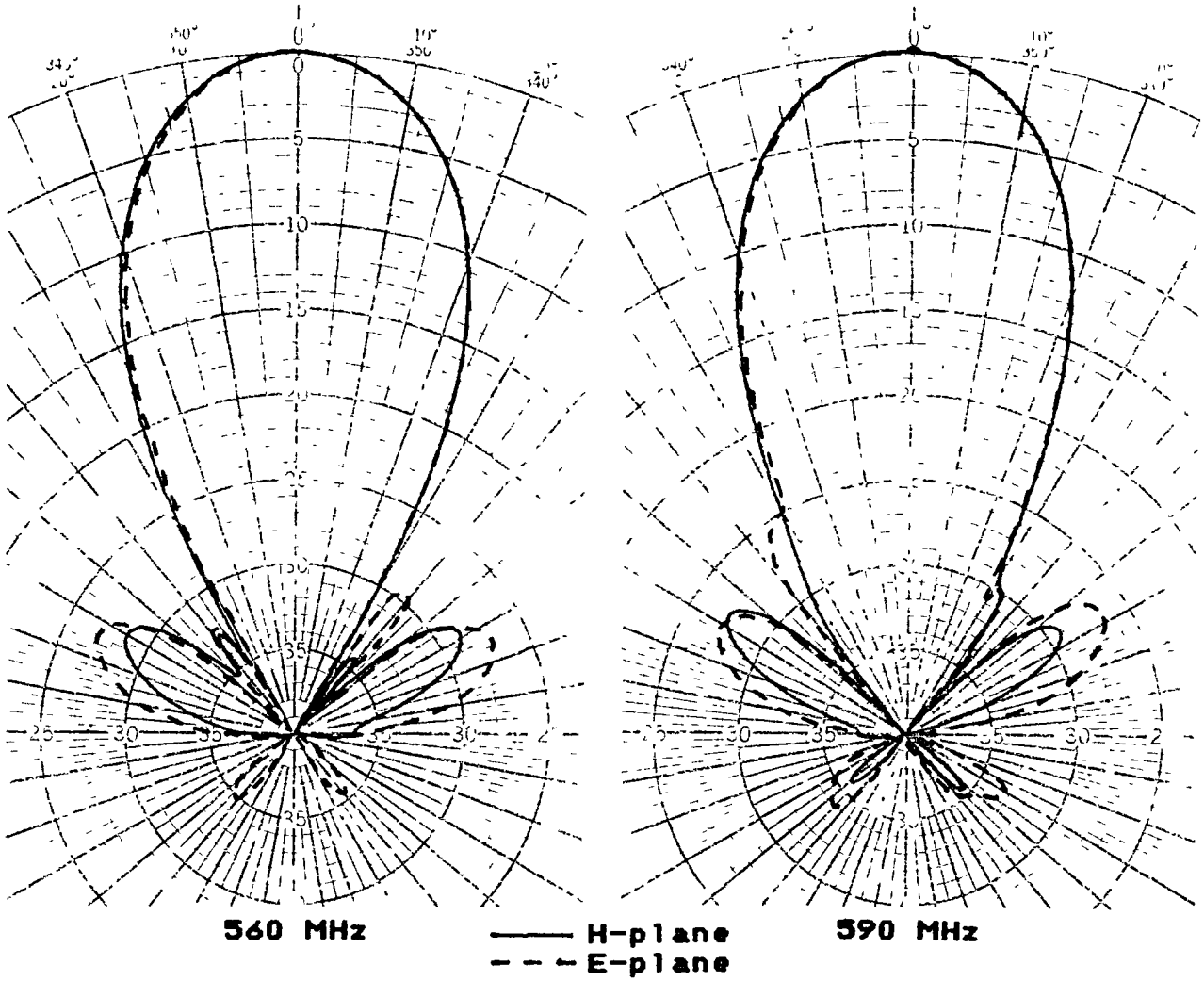

Figure 35. Measured radiation patterns for final UHF antenna array (560 MHz and 590 MHz).

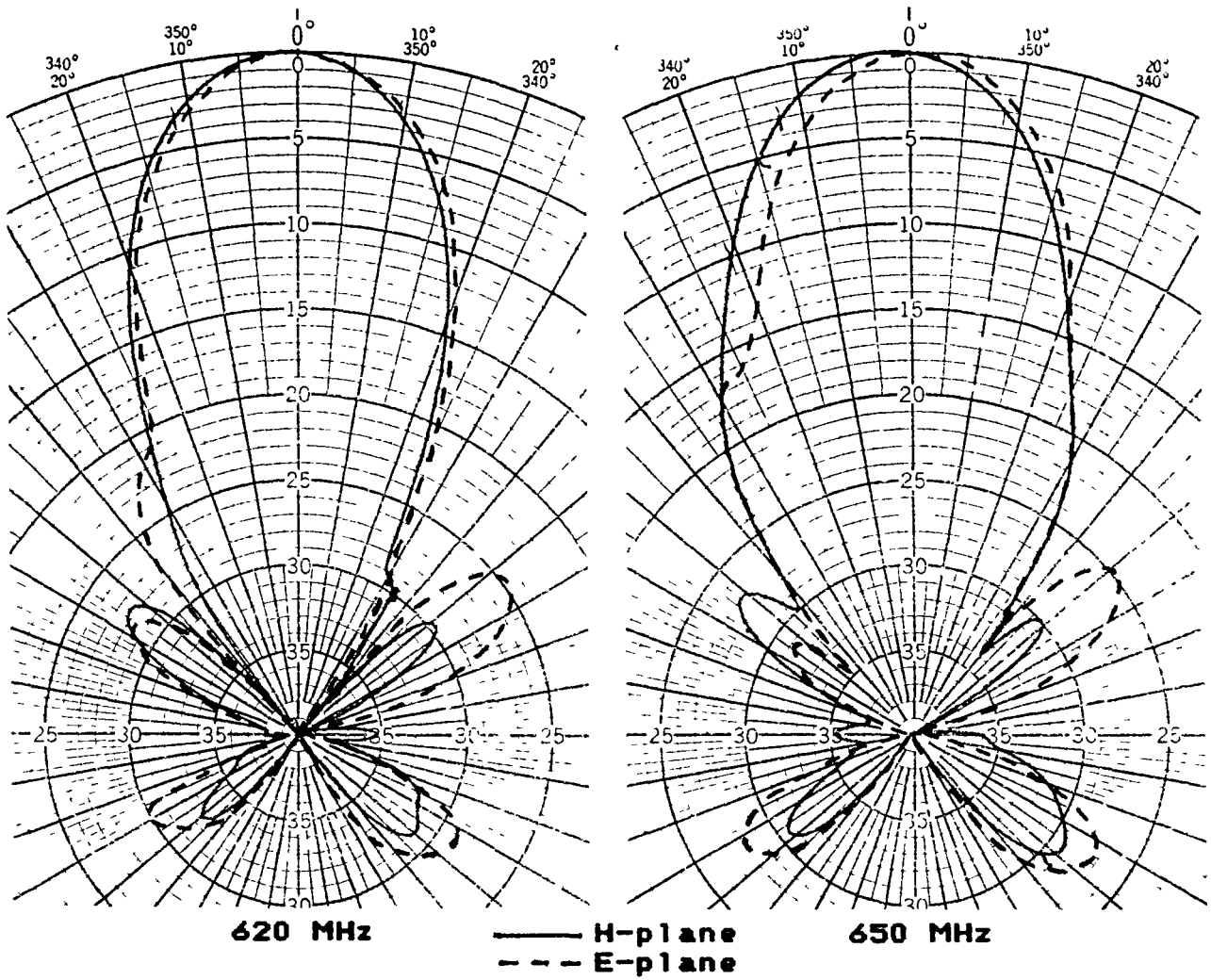

Figure 36. Measured radiation patterns for final UHF antenna array (620 MHz and 650 MHz).

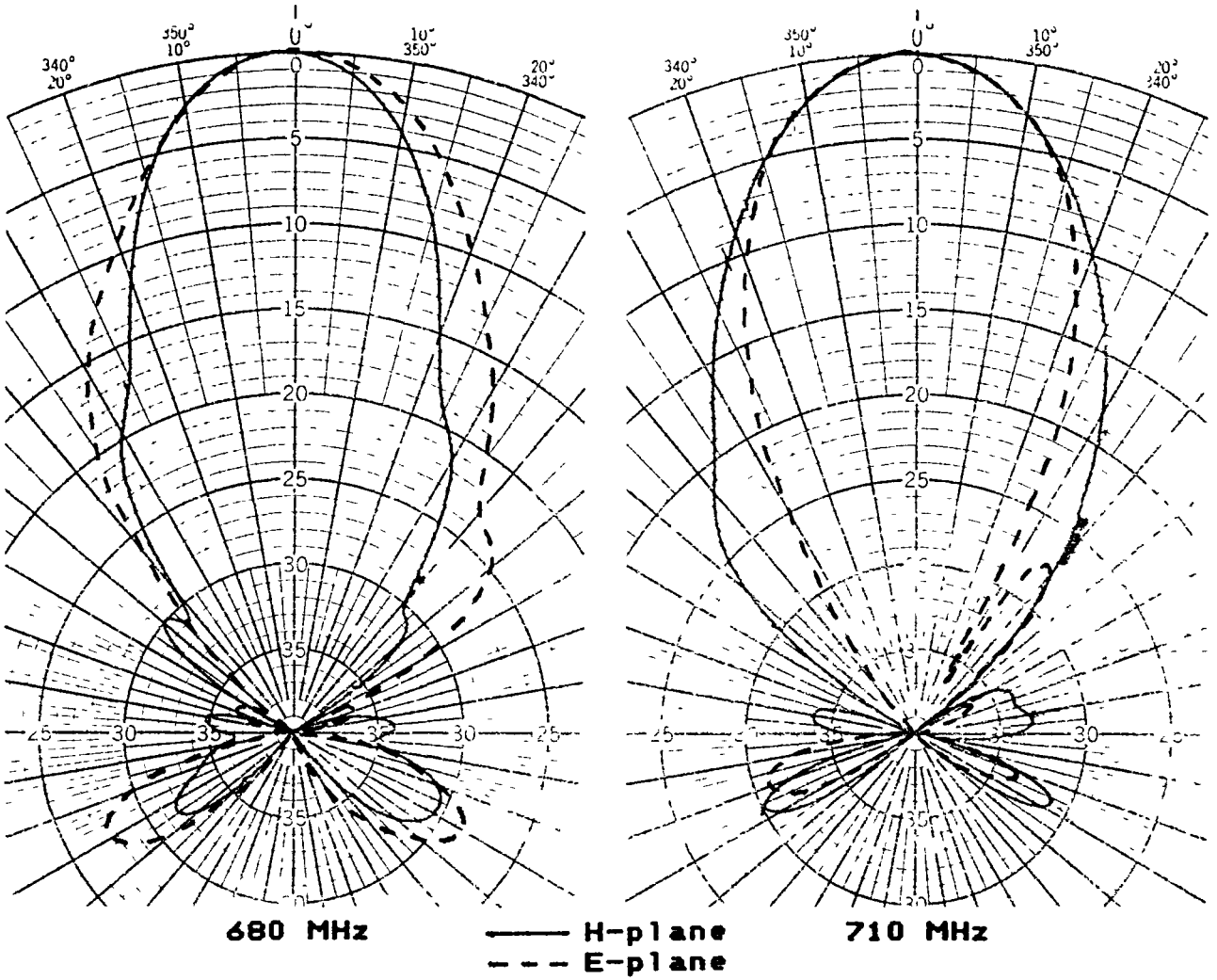

Figure 37. Measured radiation patterns for final UHF antenna array (680 MHz and 710 MHz).

1 Report No	2 Government Accession No	3 Recipient's Catalog No
NASA TM-86373		

4 Title and Subtitle	5 Report Date
BROAD-BAND UHF DIPOLE ARRAY	February 1985
	6 Performing Organization Code 146-40-13
7 Author(s)	8 Performing Organization Report No
M. C. Bailey	
9 Performing Organization Name and Address	10 Work Unit No
NASA Langley Research Center Hampton, VA 23665	11 Contract or Grant No
12 Sponsoring Agency Name and Address	13 Type of Report and Period Covered
National Aeronautics and Space Administration Washington, DC 20546	Technical Memorandum
	14 Sponsoring Agency Code

15 Supplementary Notes

16 Abstract

A 6X6 array of fan-dipoles has been designed to operate in the 510 to 660 MHz frequency range for aircraft flight test and evaluation of a UHF radiometer system. Details of a broad-band dipole design operating near the first resonance is described. Measured VSWR and radiation patterns for the dipole array demonstrate achievable bandwidths in the 35 to 40 percent range.

17 Key Words (Suggested by Author(s))	18 Distribution Statement
Antennas Array Dipole Bandwidth UHF	Unclassified - Unlimited Subject Category 32

19 Security Classif (of this report)	20 Security Classif (of this page)	21 No of Pages	22 Price
Unclassified	Unclassified	46	A03

N-305

For sale by the National Technical Information Service, Springfield, Virginia 22161

NASA-Langley, 1984

End of Document